Cell Stem Cell

Article

ADAR1-Dependent RNA Editing Promotes MET and iPSC Reprogramming by Alleviating ER Stress

Graphical Abstract

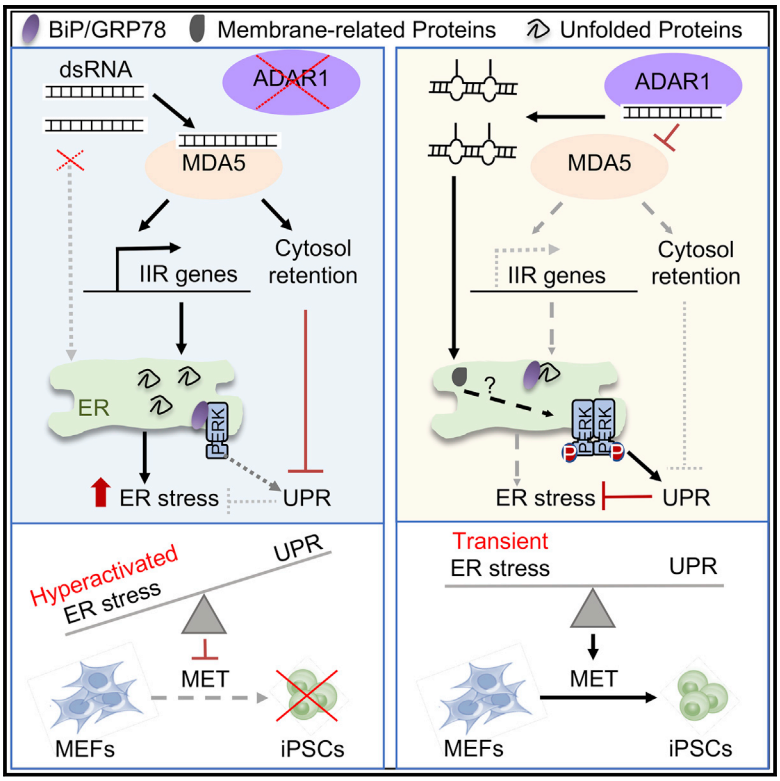

Highlights

- A-to-I RNA editing by ADAR1 is essential for epithelial cell fate acquisition
- ADAR1 loss induces ER stress that abrogates MET and hinders iPSC reprogramming
- MDA5 is required to trigger IIR and ER stress responses in the absence of A-to-I editing
- RNA editing regulates dsRNA compartmentalization and proper UPR function

Authors

Diana Guallar, Alejandro Fuentes-Iglesias, Yara Souto, ..., Carl R. Walkley, Jianlong Wang, Miguel Fidalgo

Correspondence

diana.guallar@usc.es (D.G.), jw3925@cumc.columbia.edu (J.W.), miguel.fidalgo@usc.es (M.F.)

In Brief

Guallar et al. demonstrate that RNA editing by ADAR1 safeguards mesenchymal-to-epithelial transition during reprogramming. ADAR1 orchestrates cell fate decisions by limiting MDA5 sensing of double-strand-containing RNAs encoding membrane-associated proteins and, by doing so, influences the balance between ER stress/UPR and IIR in promoting somatic cell reprogramming.

Guallar et al., 2020, Cell Stem Cell *27*, 1–15
August 6, 2020
https://doi.org/10.1016/j.stem.2020.04.016

CellPress

Please cite this article in press as: Guallar et al., ADAR1-Dependent RNA Editing Promotes MET and iPSC Reprogramming by Alleviating ER Stress, Cell Stem Cell (2020), https://doi.org/10.1016/j.stem.2020.04.016

Cell Stem Cell

CellPress

Article

ADAR1-Dependent RNA Editing Promotes MET and iPSC Reprogramming by Alleviating ER Stress

Diana Guallar,[1,2,15,*] Alejandro Fuentes-Iglesias,[1,3,15] Yara Souto,[1,3] Cristina Ameneiro,[1,3] Oscar Freire-Agulleiro,[1,3,4] Jose Angel Pardavila,[1,3] Adriana Escudero,[1,3] Vera Garcia-Outeiral,[1,3] Tiago Moreira,[1] Carmen Saenz,[5] Heng Xiong,[6,7] Dongbing Liu,[6,7] Shidi Xiao,[6,8] Yong Hou,[6,7] Kui Wu,[6,7] Daniel Torrecilla,[1] Jochen C. Hartner,[9] Miguel G. Blanco,[2] Leo J. Lee,[6,10] Miguel López,[1,3,4] Carl R. Walkley,[11,12,13] Jianlong Wang,[5,14,16,*] and Miguel Fidalgo[1,3,*]

[1]Center for Research in Molecular Medicine and Chronic Diseases (CiMUS), Universidade de Santiago de Compostela (USC)-Health Research Institute (IDIS), Santiago de Compostela 15782, Spain

[2]Department of Biochemistry and Molecular Biology, USC, Santiago de Compostela 15782, Spain

[3]Department of Physiology, USC, Santiago de Compostela 15782, Spain

[4]NeurObesity Group & CIBER Fisiopatología de la Obesidad y Nutrición (CIBEROBN), Santiago de Compostela 15706, Spain

[5]The Black Family Stem Cell Institute, Department of Cell, Developmental and Regenerative Biology, Icahn School of Medicine at Mount Sinai, New York, NY 10029, USA

[6]BGI-Shenzhen, Shenzhen 518083, China

[7]China National GeneBank-Shenzhen, BGI-Shenzhen, Shenzhen 518083, China

[8]Hubei Key Laboratory of Agricultural Bioinformatics, College of Informatics, Huazhong Agricultural University, Wuhan 430070, China

[9]Horizon Discovery, Cambridge Research Park, Cambridge CB25 9TL, UK

[10]Department of Electrical and Computer Engineering, Donnelly Centre for Cellular and Biomolecular Research, University of Toronto, Toronto, ON M5S 3G4, Canada

[11]St. Vincent's Institute of Medical Research, Fitzroy, VIC 3065, Australia

[12]Department of Medicine, St. Vincent's Hospital, University of Melbourne, Fitzroy, VIC 3065, Australia

[13]Mary MacKillop Institute for Health Research, Australian Catholic University, Melbourne, VIC 3000, Australia

[14]Department of Medicine, Columbia Center for Human Development, Columbia University Irving Medical Center, New York, NY 10032, USA

[15]These authors contributed equally

[16]Lead Contact

*Correspondence: diana.guallar@usc.es (D.G.), jw3925@cumc.columbia.edu (J.W.), miguel.fidalgo@usc.es (M.F.)

https://doi.org/10.1016/j.stem.2020.04.016

SUMMARY

RNA editing of adenosine to inosine (A to I) is catalyzed by ADAR1 and dramatically alters the cellular transcriptome, although its functional roles in somatic cell reprogramming are largely unexplored. Here, we show that loss of ADAR1-mediated A-to-I editing disrupts mesenchymal-to-epithelial transition (MET) during induced pluripotent stem cell (iPSC) reprogramming and impedes acquisition of induced pluripotency. Using chemical and genetic approaches, we show that absence of ADAR1-dependent RNA editing induces aberrant innate immune responses through the double-stranded RNA (dsRNA) sensor MDA5, unleashing endoplasmic reticulum (ER) stress and hindering epithelial fate acquisition. We found that A-to-I editing impedes MDA5 sensing and sequestration of dsRNAs encoding membrane proteins, which promote ER homeostasis by activating the PERK-dependent unfolded protein response pathway to consequently facilitate MET. This study therefore establishes a critical role for ADAR1 and its A-to-I editing activity during cell fate transitions and delineates a key regulatory layer underlying MET to control efficient reprogramming.

INTRODUCTION

Chemical modifications on RNA allow rapid cellular responses by modulating transcriptional diversity in response to internal or external stimuli (Frye et al., 2018; Roundtree et al., 2017), but the contribution of this new regulatory layer to cell fate specification remains incompletely understood.

Adenosine-to-inosine (A-to-I) deamination in RNA is among the most abundant RNA modifications in mammalian cells, and it can greatly affect the transcriptome by altering mRNA coding potential, modifying RNA structure, and regulating its localization (Walkley and Li, 2017). Mammals possess three adenosine deaminase acting on RNA (ADAR) proteins, ADAR1, ADAR2, and ADAR3, among which only the first two are known to exert catalytic activity on RNA (Chen et al., 2000; Oakes et al., 2017). ADAR1-deficient mice display a profound deregulation of genes related to the innate immune response (IIR) and embryonic lethality at embryonic day 11.5 (E11.5) to E13.5 (Hartner et al., 2009; Lamers et al., 2019), which can be rescued with the deletion of the cytosolic double-stranded RNA (dsRNA) sensor

Please cite this article in press as: Guallar et al., ADAR1-Dependent RNA Editing Promotes MET and iPSC Reprogramming by Alleviating ER Stress, Cell Stem Cell (2020), https://doi.org/10.1016/j.stem.2020.04.016

MDA5 or its downstream effector MAVS (Liddicoat et al., 2015; Mannion et al., 2014; Pestal et al., 2015).

Immune responses interact with other cellular stress responses including endoplasmic reticulum (ER) stress, which results from the accumulation of misfolded or unfolded proteins in the ER lumen (Bettigole and Glimcher, 2015; So, 2018). ER stress activates the unfolded protein response (UPR), a conserved eukaryotic stress response mechanism mediated by IRE1/PERK/ATF6 signaling pathways, to restore ER homeostasis (Wang and Kaufman, 2016). While ER stress and the UPR have been involved in cell fate decisions in a cell-context-dependent manner (Hetz, 2012; Wang and Kaufman, 2016), how the IIR modulator ADAR1 and its RNA editing activity may functionally intersect with these pathways to regulate ER function and cell fate determination is currently unknown.

The generation of induced pluripotent stem cells (iPSCs) through somatic cell reprogramming with four transcription factors (i.e., *Oct4*, *Sox2*, *Klf4*, and *c-Myc*; also known as OSKM) (Takahashi et al., 2007; Takahashi and Yamanaka, 2006) represents a valuable approach to investigate general mechanisms of cell fate determination. Under standard conditions, the OSKM reprogramming of fibroblasts involves an initial mesenchymal-to-epithelial transition (MET) (Li et al., 2010; Samavarchi-Tehrani et al., 2010) and is generally slow and inefficient owing to the existence of barriers to cell fate changes (Apostolou and Stadtfeld, 2018; Haridhasapavalan et al., 2020). While transcriptional and epigenetic barriers have been extensively examined and identified (Apostolou and Stadtfeld, 2018; Haridhasapavalan et al., 2020), the role of RNA modifications (Aguilo et al., 2015; Chen et al., 2015a) in cell fate control has just begun to be appreciated.

In this study, we found that absence of ADAR1-mediated A-to-I editing in reprogramming enabled MDA5 sensing and cytoplasmic retention of double-stranded RNAs (dsRNAs) encoding membrane-associated proteins, which led to the upregulation of IIR, ER stress, and defective activation of the PERK signaling pathway of the UPR. Consequently, the transient ER stress that we found associated with MET during reprogramming becomes hyperactivated upon the loss of ADAR1, leading to the inhibition of epithelial cell fate specification and compromised iPSC generation.

RESULTS

ADAR1 Catalytic Activity Is Required for Somatic Cell Reprogramming

To investigate whether RNA editing participates in the somatic cell reprogramming process, we first employed an unbiased *in silico* approach using published RNA-sequencing (RNA-seq) datasets to compare A-to-I editing sites in somatic mouse embryonic fibroblasts (MEFs) and pluripotent iPSCs. Interestingly, the editing profiles of each cell line were sufficient to segregate the samples according to their cellular identity (Figures 1A and S1A–S1C) with a higher editing frequency in MEFs than iPSCs (Figure 1B), which was further confirmed using an A-to-I reporter system (Figures 1C and 1D).

We next examined the effect of transient suppression of ADAR1 or ADAR2 in the acquisition of the pluripotent cell identity using MEFs harboring a green fluorescent protein (GFP) reporter under the control of the *Pou5f1* (aka *Oct4*) gene (*Pou5f1*-GFP) transduced with the OSKM cassette. Intriguingly, we found that knockdown of *Adar1*, but not *Adar2*, was sufficient to significantly abrogate the generation of GFP^+ iPSC colonies compared with a control small hairpin RNA (shRNA) targeting luciferase (Figures 1E, S1D, and S1E), concomitant with downregulation of the pluripotency genes (Figure S1F). Notably, the few iPSC colonies that arose from sh*Adar1*-transduced MEFs did not have reduced *Adar1* expression (Figure S1G). The impairment of somatic cell reprogramming by *Adar1* depletion was due neither to the delay in iPSC formation (Figure S1H), nor to the reprogramming barrier function of cell contact inhibition despite a slight increase of MEF proliferation upon Adar1 depletion (Figures S1I and S1J). Notably, the ADAR1 requirement for reprogramming was also conserved in the human system (Figure 1F). In addition, knockdown of *Adar1* not only abrogated OSKM reprogramming of peripheral blood mononuclear cells (PBMCs) (Figure S1K) but also significantly reduced reprogramming of MEFs transduced with Pei's seven-factor (7F) cocktail (i.e., *Jdp2*, *Jhdm1b*, *Mkk6*, *Glis1*, *Nanog*, *Esrrb*, and *Sall4*) (Wang et al., 2019) (Figure 1G). Furthermore, depletion of *Adar1* compromised the direct reprogramming of fibroblasts into induced neurons (Chanda et al., 2014) (Figure 1H). Altogether, these data support a critical role for ADAR1 in reprogramming cell fates that is not restricted to OSKM reprogramming cocktail or fibroblasts.

To address the specific contribution of A-to-I editing activity to cell fate transitions during reprogramming, we derived MEFs from $Adar1^{Fl/Fl}$ and $Adar1^{Fl/E861A}$ mice with $CreER^{T2}$ knocked into Rosa26 locus (Hartner et al., 2009; Liddicoat et al., 2015). Treatment with 4-hydroxytamoxifen (4OHT) renders these mice or cells either *Adar1* null (for $Adar1^{Fl/Fl}$) or only expressing editing-deficient $Adar1^{E861A}$ (for $Adar1^{Fl/E861A}$) (Figure S1L). In line with our shRNA experiments, genetic depletion of *Adar1* impaired the formation of alkaline-phosphatase-positive (AP^+) colonies (Figure 1I), and more importantly, the editing mutant (MUT) mirrored the effects of ADAR1 null with compromised somatic cell reprogramming (Figure 1J). Furthermore, the reprogramming defects elicited by ADAR1 deficiency (i.e., $Adar1^{Fl/Fl}$ + 4OHT) can only be rescued by the ectopic expression of a wild-type (WT), but not editing mutant (E861A), ADAR1 (Figure 1I). Altogether, these data establish the essential role of A-to-I editing activity for pluripotency acquisition in reprogramming.

Absence of RNA Editing by ADAR1 Prevents MET during Reprogramming

To investigate the time window when ADAR1 activity is required during the multistep reprogramming process, we first evaluated iPSC formation at day 14 and observed that *Adar1* depletion failed not only to induce the expression of the pluripotency regulator NANOG and the epithelial marker CDH1 (aka E-CADHERIN) but also to suppress the fibroblast mesenchymal factor CDH2 (Figure 2A), suggesting a possible defect on MET. Supporting this, gene expression dynamics showed that loss of *Adar1* resulted in reduced transcriptional activation of epithelial genes and inefficient shutdown of mesenchymal genes (Figures 2B and S2A). Immunofluorescence analysis at day 7 for early reprogramming markers (i.e., CDH1 and SSEA1) further

Please cite this article in press as: Guallar et al., ADAR1-Dependent RNA Editing Promotes MET and iPSC Reprogramming by Alleviating ER Stress, Cell Stem Cell (2020), https://doi.org/10.1016/j.stem.2020.04.016

CellPress

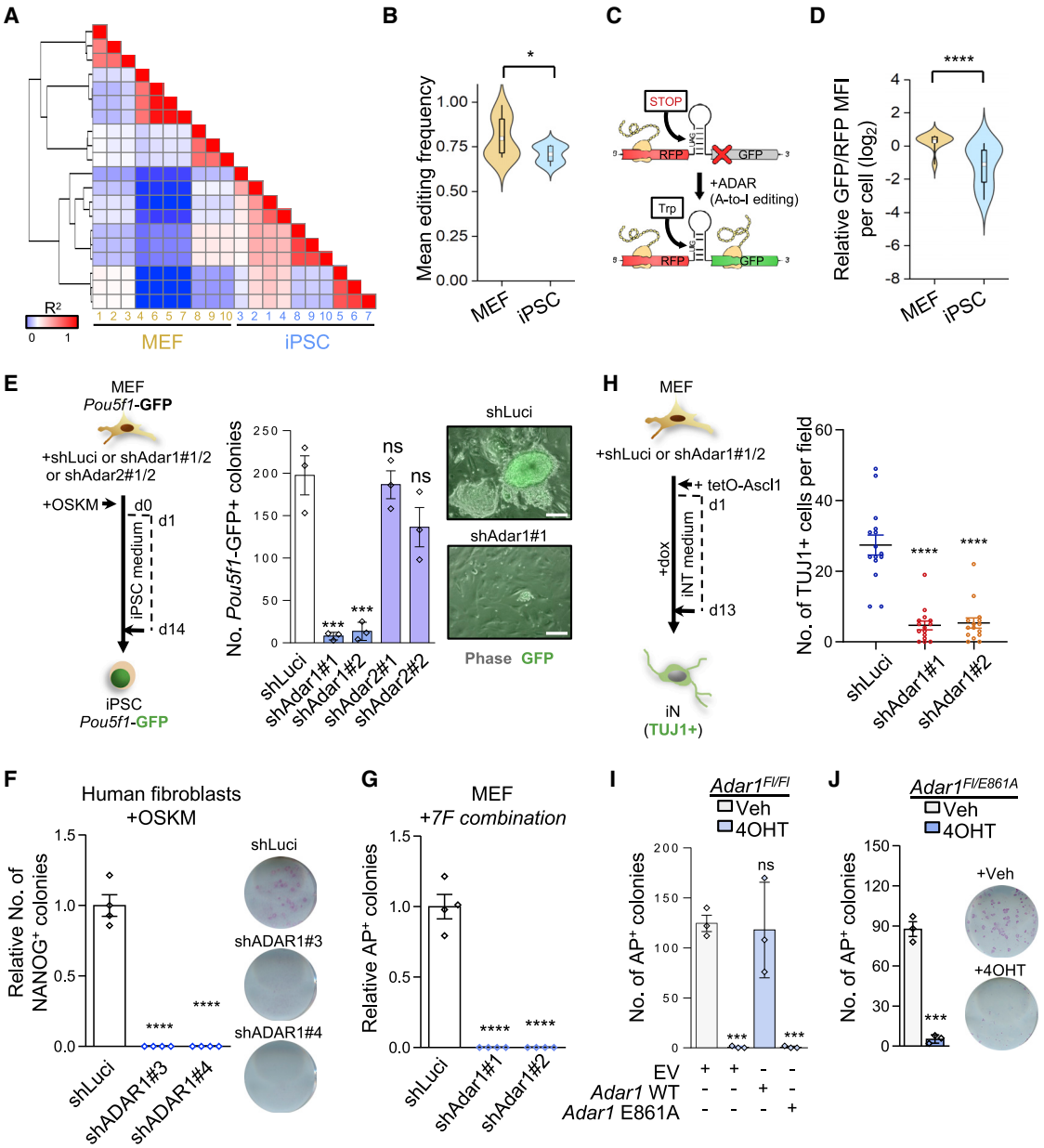

Figure 1. ADAR1 Catalytic Activity Is Required for Reprogramming of Fibroblasts

(A) Heatmap and dendrogram of Pearson correlations on the editing levels of 10 MEF and 10 iPSC cell lines.

(B) Mean editing frequency in MEFs and iPSCs.

(C) Schematic depiction of the A-to-I reporter.

(D) Relative GFP/RFP mean fluorescence intensity (MFI) in MEFs and iPSCs transfected with the editing reporter.

(E) Left: schematic depiction of the reprogramming strategy used. Right: number of *Pou5f1*-GFP$^+$ iPSC colonies and representative images. Scale bar represents 300 μm.

(F) Relative number of NANOG-positive iPSC colonies after reprogramming of normal human lung fibroblasts.

(G) Relative number of AP$^+$ iPSC colonies at day 18 obtained after reprogramming of MEFs with the 7F cocktail.

(H) Left: schematic depiction of the transdifferentiation strategy used to generate induced neurons (iN) by overexpression of *Ascl1* in MEFs. Right: number of TUJ1-positive neurons obtained.

(I) Number of AP$^+$ iPSC colonies after 14 days of reprogramming.

(J) Number of AP$^+$ iPSC colonies and representative images of AP-stained wells at day 14 of reprogramming.

In (B) and (D), the plots display the mean, interquartile range, 5th–95th confidence interval range, and the probability density of the data. One-way ANOVA with Tukey's post-test was performed. In (E)–(J), data are shown as mean ± SEM (n = 3 independent experiments unless otherwise indicated). Two-tailed Student's t test was performed. ***p < 0.001; ****p < 0.0001; ns, not significant. See also Figure S1.

Please cite this article in press as: Guallar et al., ADAR1-Dependent RNA Editing Promotes MET and iPSC Reprogramming by Alleviating ER Stress, Cell Stem Cell (2020), https://doi.org/10.1016/j.stem.2020.04.016

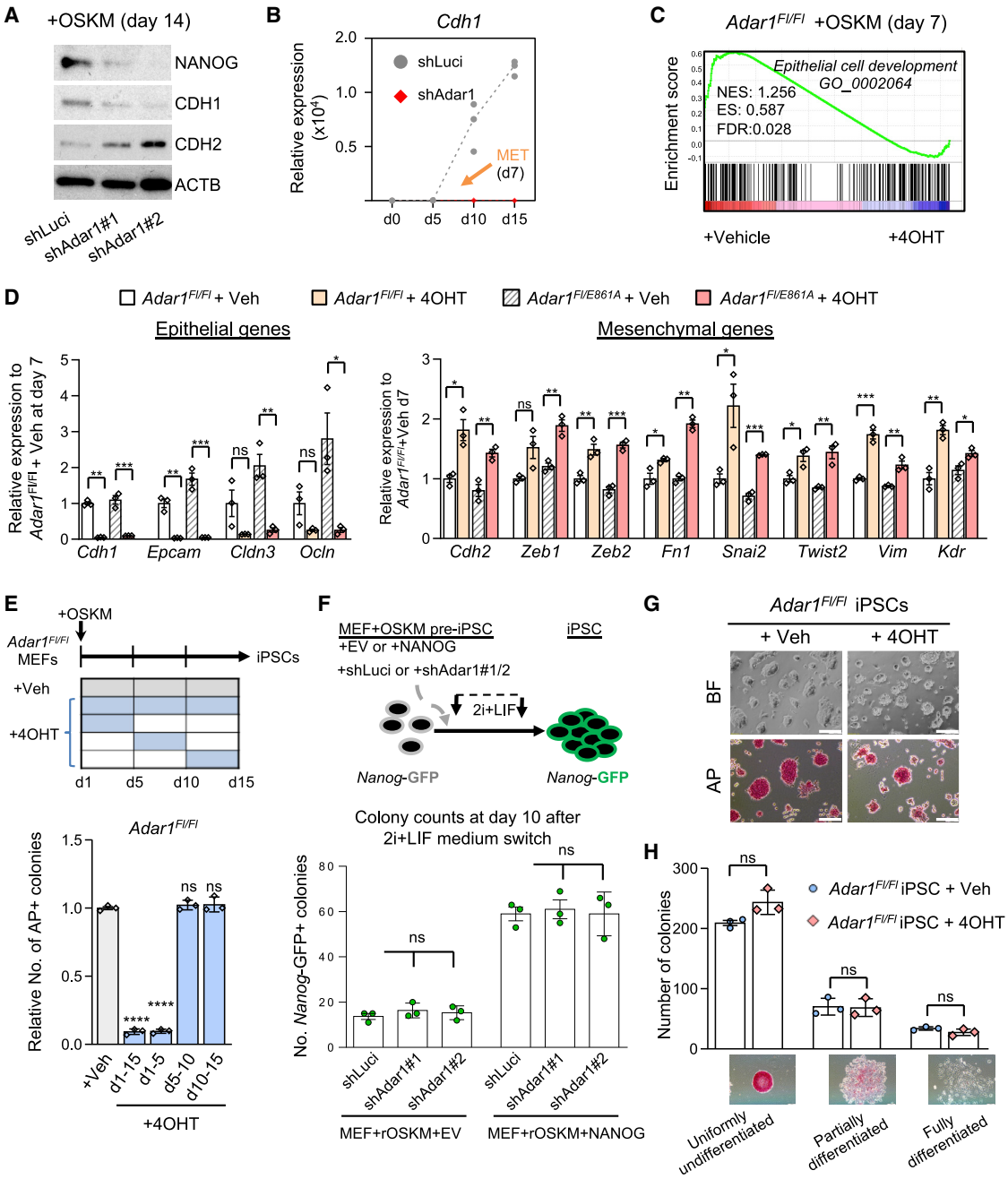

Figure 2. RNA Editing by ADAR1 Is Essential for Epithelial Cell Fate Acquisition during Reprogramming

(A) Western blot of NANOG, CDH1, and CDH2 proteins in MEFs transduced with OSKM and the indicated shRNAs. ACTB was used as a loading control.

(B) Relative expression of *Cdh1* during MEF reprogramming (n = 3 independent experiments).

(C) GSEA of epithelial cell development signatures at day 7 of reprogramming.

(D) Relative expression of epithelial and mesenchymal markers in the indicated cell lines and treatments.

(E) Top: illustration of indicated treatments at different time windows during reprogramming of *Adar1*$^{Fl/Fl}$ MEFs. Bottom: relative number of AP^{+} iPSC colonies obtained with the indicated treatments.

(F) Top: schematic depiction of epithelial MEF+OSKM pre-iPSC reprogramming strategy. Bottom: quantification of *Nanog*-GFP^{+} iPSC colonies after 10 days of reprogramming. EV, empty vector.

(G) Representative bright-field (BF) and AP-staining images of three different experiments.

(H) Quantification of a colony formation assay with iPSCs from the indicated genotypes.

In (D)–(F) and (H), data are shown as mean ± SEM (n = 3 independent experiments). Two-tailed Student's t test was performed. *p < 0.05; **p < 0.01; ***p < 0.001; ****p < 0.0001; ns, not significant. See also Figure S2.

Please cite this article in press as: Guallar et al., ADAR1-Dependent RNA Editing Promotes MET and iPSC Reprogramming by Alleviating ER Stress, Cell Stem Cell (2020), https://doi.org/10.1016/j.stem.2020.04.016

confirmed the requirement of ADAR1 for MET during iPSC formation (Figure S2B). Likewise, genetic depletion of ADAR1 demonstrated that ADAR1 plays a pivotal role in the transcriptional activation of the epithelial program in this initiation phase of reprogramming (Figure 2C). Importantly, presence of editing-deficient ADAR1 protein (*Adar1*^{E861A}) was not sufficient to restore proper MET (Figure 2D).

Taken together, these results establish an essential role for RNA A-to-I editing activity of ADAR1 in the earliest phase of reprogramming that involves a requisite MET.

ADAR1 Function Is Dispensable at the Late Stage of Reprogramming and for iPSC Maintenance

We then addressed potential roles of ADAR1 beyond MET during iPSC generation. While confirming the requisite role of ADAR1 at the earliest stage of reprogramming coinciding with MET (i.e., days 1–5) (Figure 2E), we observed, however, no significant differences in iPSC formation between vehicle (Veh)- or 4OHT-treated *Adar1*$^{Fl/Fl}$ MEFs at later time points (Figure 2E) when the epithelial fate has already been established. Such an ADAR1 dispensability after MET was further supported by nonsignificant effects of ADAR1 depletion on reprogramming to iPSCs of epithelial intermediate state cells (aka pre-iPSC) (Costa et al., 2013) (Figure 2F) or somatic epithelial normal murine mammary gland cells (Figures S2C and S2D).

Next, we investigated whether depletion of *Adar1* influences the late stabilization phase, when reprogrammed cells have activated the pluripotency gene program and successfully transited to iPSCs (Plath and Lowry, 2011). For this, we established stable *Adar1*$^{Fl/Fl}$ iPSCs followed by 4OHT treatment over a period of >10 passages to deplete ADAR1. We found that *Adar1* knockout (KO) cells maintained a normal undifferentiated iPSC morphology with stem-cell-specific alkaline phosphatase (AP) positivity (Figure 2G). Colony-formation assays (Figure 2H) and gene expression analyses (Figures S2E–S2G) revealed no significant differences in self-renewal between *Adar1* KO and WT iPSCs. Of note, *Adar1* KO iPSCs are compromised in differentiation toward mesoderm and endoderm lineages (Figures S2H and S2I).

Together, these results support a nonessential role for ADAR1 in later stages of reprogramming beyond MET and in the maintenance of iPSCs with an epithelial cell identity.

Absence of A-to-I Editing Hyperactivates ER Stress

To gain further insight into the mechanisms of ADAR1 and its editing activity on MET, we performed transcriptional profiling at day 7 of OSKM reprogramming of *Adar1*$^{Fl/Fl}$ and *Adar1*$^{Fl/E861A}$ MEFs treated with vehicle or 4OHT. We identified 668 upregulated and 1,162 downregulated genes (fold change [FC] > 2) in the absence of ADAR1-mediated RNA editing (Figures 3A and S3A–S3C; Table S1) with the enrichment of "response to stress" and "endoplasmic reticulum (ER)" Gene Ontology (GO) categories (Figure 3B). Considering that ER-translated membrane proteins represent a significant fraction of the total proteome (Diehn et al., 2000; Reid and Nicchitta, 2012) and the profound morphological changes and proteomic rewiring that take place during MET (Hansson et al., 2012; Li et al., 2010; Samavarchi-Tehrani et al., 2010), we reasoned that the ER protein-folding capacity might be overloaded during reprogramming leading to ER stress and that a mechanism such as UPR must be in place to restore ER functionality and facilitate epithelial fate acquisition. Indeed, we observed the upregulation of UPR-related genes during a short time window coincident with MET, indicative of a "transient ER stress" that is compatible with epithelial gene activation during normal reprogramming (Figure 3C). More importantly, we found a significant upregulation of genes related to ER stress and the UPR at the MET stage during reprogramming of MEFs deficient for ADAR1 or its editing activity, while housekeeping genes remained unchanged (Figures 3D and 3E). These results suggest that the observed "hyperactivated ER stress" upon the loss of ADAR1 or its editing activity may be detrimental to MET, which was confirmed by our following experiments.

First, we ectopically induced ER stress with tunicamycin and thapsigargin and found that acquisition of epithelial cell identity and reprogramming were significantly compromised (Figures 3F and 3G). Second, we performed OSKM-mediated MEF reprogramming with forced expression of a dominant-negative isoform of the chaperone GRP78 (aka BiP or HSPA5), which acts upstream of the UPR to modulate ER (Hendershot et al., 1995), and found that this UPR disruption also compromised reprogramming (Figure S3D). Third, we employed genetical interventions to promote UPR function by ectopic expression of WT GRP78 or ATF4, which led to significantly increased reprogramming efficiency (Figure S3E). In contrast, knockdown of UPR-related genes (i.e., *Atf6*, *Ire1*, and *Atf3*) severely compromised iPSC generation (Figure S3F). Fourth, we observed that induction of ER stress with tunicamycin or GRP78DN mainly abrogated reprogramming of *Adar1* WT cells at early, but not later, phases of iPSC generation, when MET takes place (Figure S3G). Fifth, we treated *Adar1* WT MEFs with the ER stress inhibitors salubrinal (Boyce et al., 2005) and azoramide (Fu et al., 2015) and observed enhanced MET and reprogramming (Figures S3H and S3I). Lastly, we used same ER stress inhibitors to curtail or suppress the hyperactivated ER stress during reprogramming of *Adar1* editing activity-deficient MEFs and observed the rescue of both epithelial gene activation (Figure 3H) and iPSC formation (Figure 3I).

These results together establish that hyperactivated ER stress, resulting from the loss of ADAR1 RNA editing activity, acts as an intrinsic barrier that preserves the mesenchymal phenotype of fibroblasts and hampers MET during reprogramming to epithelial fated iPSCs.

MDA5 Is Required to Hyperactivate ER Stress Response in the Absence of A-to-I Editing

To delineate the molecular events leading to the hyperactivated ER stress during reprogramming in the absence of ADAR1, we first asked whether aberrant IIRs observed in mutant mouse (Hartner et al., 2009) and human Aicardi-Goutières syndrome (Rice et al., 2012; Rice et al., 2017) are also present at MET during MEF reprogramming to iPSCs. Gene set enrichment analysis (GSEA) and GO analysis revealed the upregulation of gene signatures related to innate immune/interferon responses (Figures 4A and S4A). Notably, among the most differentially expressed genes, 70 IIR-related markers were significantly upregulated in both *Adar1* KO and editing mutant cells at day 7 of reprogramming (Figures 4B and S4B). Of note, a transient activation of IIR concomitantly with UPR activation during

Please cite this article in press as: Guallar et al., ADAR1-Dependent RNA Editing Promotes MET and iPSC Reprogramming by Alleviating ER Stress, Cell Stem Cell (2020), https://doi.org/10.1016/j.stem.2020.04.016

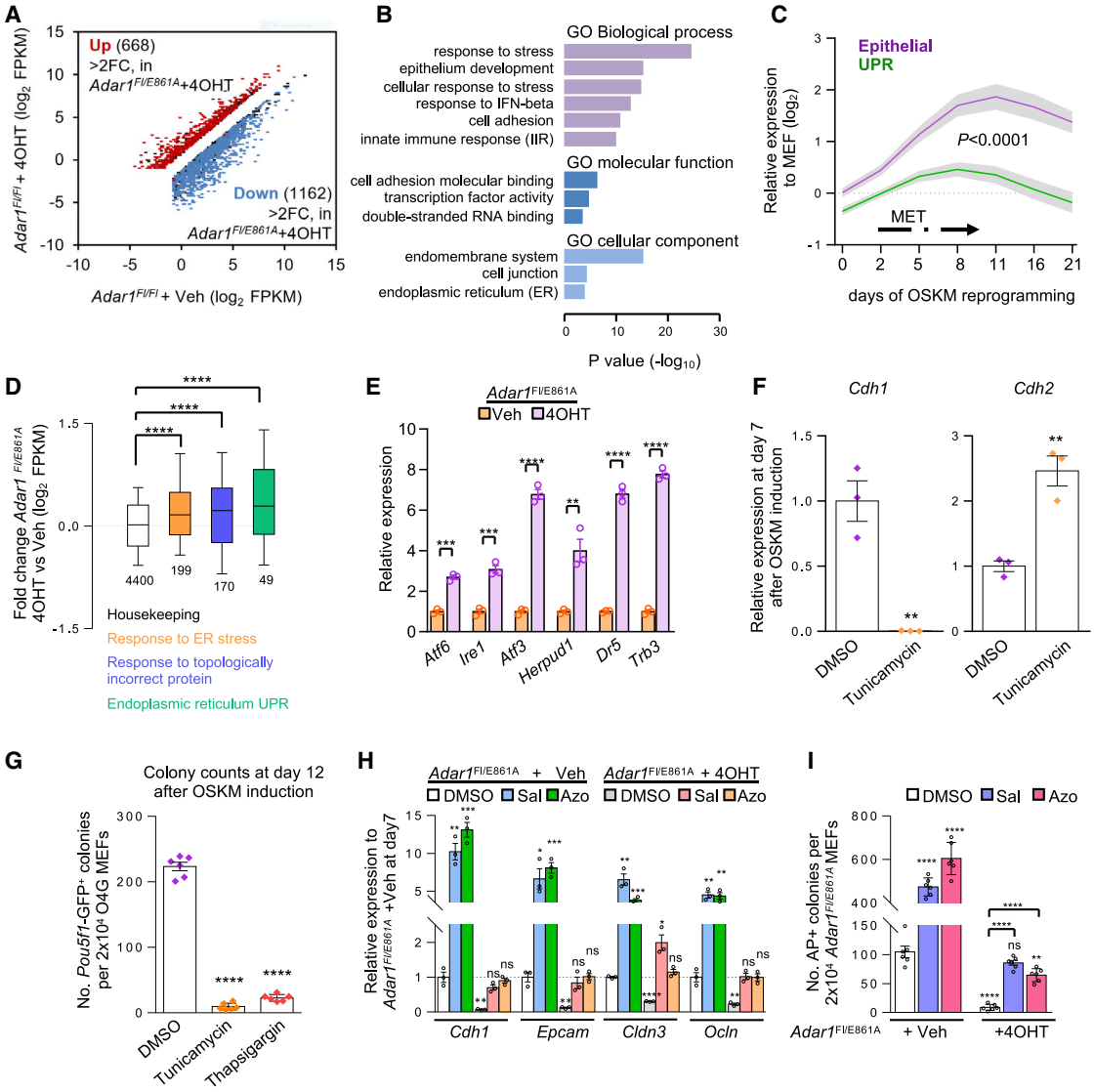

Figure 3. Absence of A-to-I Editing Promotes Endoplasmic Reticulum Stress

(A) Scatterplot of gene expression. Genes found to be upregulated or downregulated more than 2-fold (>2FC) in *Adar1*$^{FI/E861A}$ + 4OHTcells are indicated in red and blue, respectively.

(B) Representative GO categories enriched in differentially expressed genes in absence of ADAR1 catalytic activity.

(C) Relative expression of epithelial and UPR-related genes during reprogramming of MEFs with inducible OSKM expression (Samavarchi-Tehrani et al., 2010) without ADAR1 manipulation.

(D) Fold RNA expression changes of the indicated gene categories in *Adar1*$^{FI/E861A}$ + 4OHT cells compared with Veh treatment. The number of genes included in each category is indicated. Whiskers extend to the 10th–90th percentile range.

(E) Relative expression of ER-stress-related genes in the cells with the indicated treatments.

(F) Expression of *Cdh1* and *Cdh2* markers at day 7 of reprogramming after the indicated treatments.

(G) Number of *Pou5f1*-GFP^{+} iPSC colonies at day 12 of reprogramming after control (DMSO) or ER stress inducer treatment.

(H) Expression of epithelial genes in *Adar1*$^{FI/E861A}$ cells treated with control (Veh) or 4OHT and either ER stress inhibitors or a control (DMSO).

(I) Number of pluripotent AP^{+} colonies after 14 days of reprogramming, treated as in (H).

In (C) and (D), one-way ANOVA with Tukey's post-test was performed. Data in (E)–(I) are shown as the mean ± SEM, each data point represents independent experiments, and two-tailed Student's t test was performed. *p < 0.05; **p < 0.01; ***p < 0.001; ****p < 0.0001; ns, not significant. All data correspond to day 7 of reprogramming unless otherwise indicated. See also Figure S3 and Table S1.

MET was also observed in reprogramming even with a lentivirus-free transducing system (Figures 4C and S4C). Importantly, ADAR1 depletion resulted in a sustained derepression of IIR during reprogramming (Figure S4D). Furthermore, by analyzing gene interaction networks using the STRING database, we found that 94.8% of the IIR genes activated during MET were related to response to stress, membrane-bounded organelle, or both (Figure S4E).

Please cite this article in press as: Guallar et al., ADAR1-Dependent RNA Editing Promotes MET and iPSC Reprogramming by Alleviating ER Stress, Cell Stem Cell (2020), https://doi.org/10.1016/j.stem.2020.04.016

CellPress

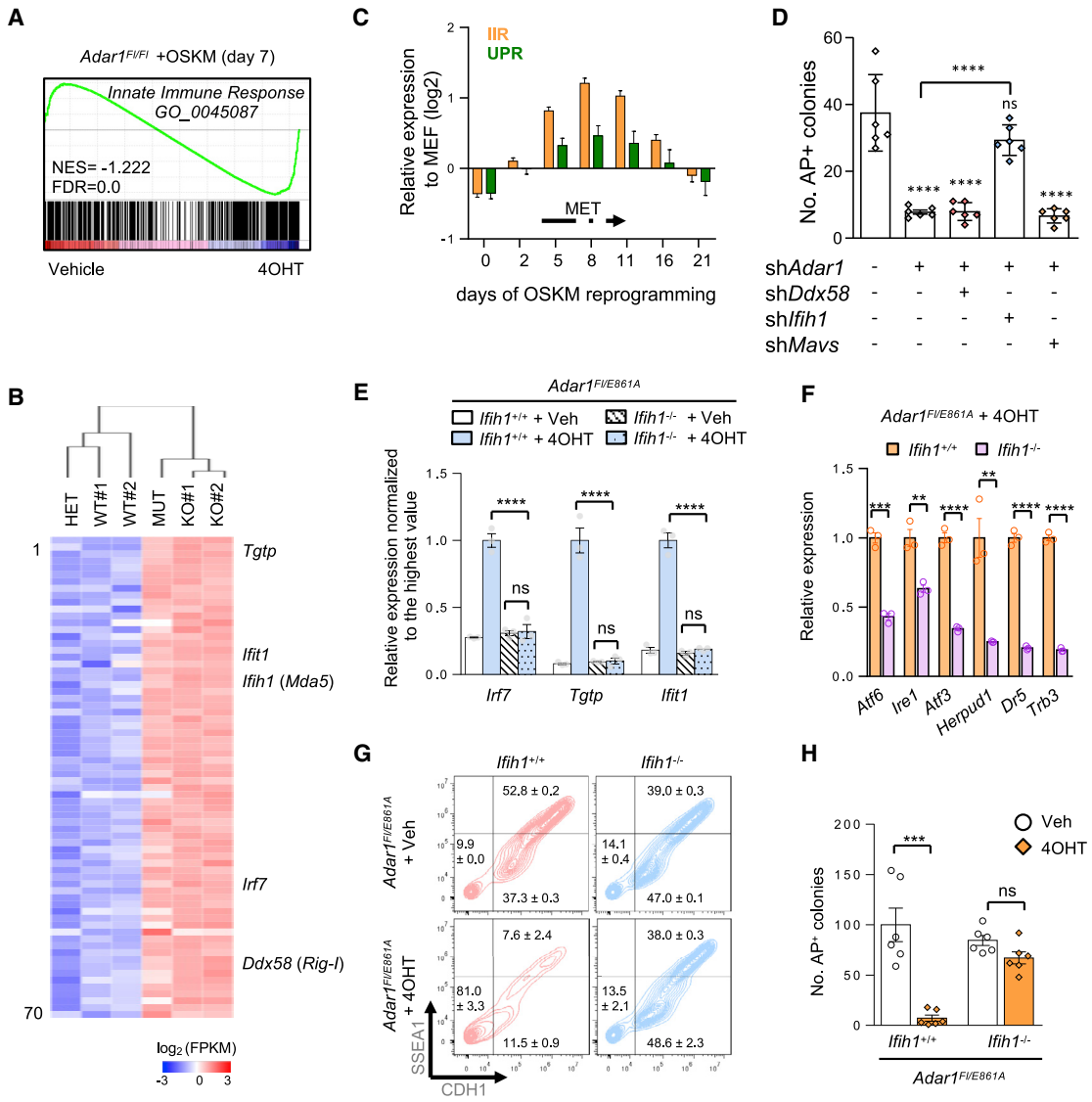

Figure 4. MDA5 Is Required to Trigger ER Stress Response in the Absence of A-to-I Editing

(A) GSEA plot showing positive correlations between ADAR1 depletion reprogramming and IIR gene signatures.

(B) Heatmap of the 70 IIR-related markers that are most differentially expressed.

(C) Relative expression of IIR and UPR genes during somatic cell reprogramming in a secondary system by inducible OSKM expression (Samavarchi-Tehrani et al., 2010).

(D) Number of AP$^+$ iPSC colonies at day 14 of reprogramming of MEFs transduced with the indicated shRNAs.

(E) Relative expression of IIR-related genes in the indicated cell lines.

(F) Relative expression of ER stress/UPR-related genes in the indicated cell lines.

(G) Flow cytometry analysis of early pluripotency (SSEA1) and epithelial (CDH1) markers.

(H) Number of AP$^+$ iPSC colonies at day 14 of reprogramming of the indicated genotypes.

Data in (D)–(F) and (H) are shown as the mean ± SEM, each data point represents independent experiments, and two-tailed Student's t test was performed. **p < 0.01; ***p < 0.001; ****p < 0.0001; ns, not significant. All data correspond to day 7 of reprogramming unless otherwise indicated. See also Figure S4.

The sustained derepression of the IIR produced by the absence of ADAR1 can be rescued by genetic deletion of MDA5 (*Ifih1* gene) or MAVS (*Mavs* gene), but not RIG-I (*Ddx58* gene) (Liddicoat et al., 2015; Mannion et al., 2014; Pestal et al., 2015). To test whether an analogous mechanism may operate during reprogramming of *Adar1*-deficient cells, we performed loss-of-function studies of both IIR transducers (*Ifih1* and *Ddx58*) and their effector (*Mavs*). In WT cells where ADAR1 is intact, we found that *Ifih1* knockdown did not affect reprogramming and that depletion of *Ddx58* and *Mavs* greatly reduced iPSC generation (Figures S4F and S4G). However, in *Adar1*-depleted cells, we observed that only knockdown of *Ifih1,* but not *Ddx58* or *Mavs*, was able to rescue efficient reprogramming (Figure 4D). In line with this finding, genetic ablation of *Ifih1*

Please cite this article in press as: Guallar et al., ADAR1-Dependent RNA Editing Promotes MET and iPSC Reprogramming by Alleviating ER Stress, Cell Stem Cell (2020), https://doi.org/10.1016/j.stem.2020.04.016

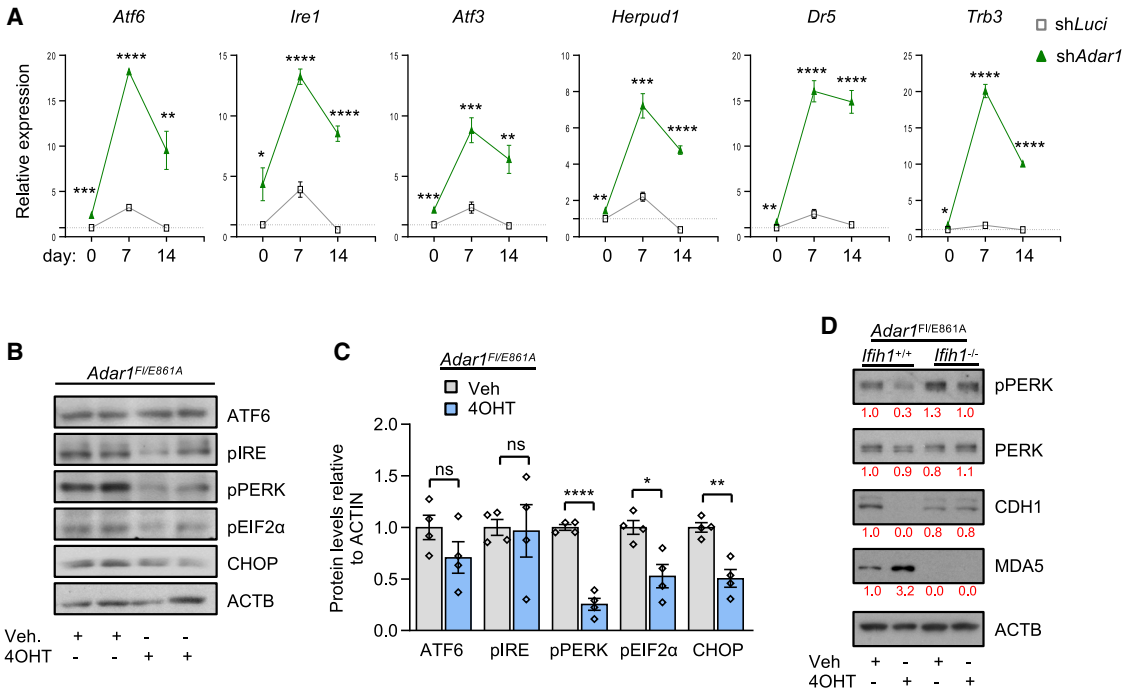

Figure 5. RNA Editing by ADAR1 Enables Efficient PERK Activation

(A) Expression of ER stress/UPR-related genes during OSKM reprogramming of MEFs (n = 3 independent experiments).

(B) Representative western blot of UPR regulators at day 7 of OSKM reprogramming of MEFs with the indicated genotypes.

(C) Quantification of four independent experiments.

(D) Western blot of pPERK, PERK, CDH1, and MDA5 at day 7 of reprogramming, treated as indicated.

In (A) and (C), data are shown as mean ± SEM. Two-tailed Student's t test was performed. *p < 0.05; **p < 0.01; ***p < 0.001; ****p < 0.0001; ns, not significant. In (B) and (D), ACTB was used as a loading control. See also Figure S5.

abrogated the observed IIR derepression (Figure S4D) in ADAR1 editing-deficient cells during MET (Figure 4E). Remarkably, we also observed that the hyperactivated ER stress genes caused by absence of ADAR1 catalytic activity was substantially reduced in MDA5 (*Ifih1*)-depleted cells (Figure 4F). Consequently, the removal of *Ifih1* was sufficient to rescue both the activation of the epithelial *Cdh1* gene during early reprogramming (Figures 4G, S4H, and S4I) and final iPSC formation (Figures 4H and S4J).

Taken together, these results demonstrate that ADAR1-dependent A-to-I RNA editing safeguards MET by restraining MDA5-mediated IIR and ER stress associated with the reprogramming process.

RNA Editing by ADAR1 Enables Efficient PERK Activation

The accumulation of misfolded proteins leading to ER stress is buffered by the activation of the UPR under both physiological and pathological conditions (Schröder and Kaufman, 2005; Wang and Kaufman, 2016) (Figure S5A, left and middle panels). Paradoxically, UPR promotes either cell survival by reducing unfolded protein load or cell death when ER stress is chronic (Hetz, 2012). However, unlike the chronic ER stress, despite the failure to downregulate ER stress/UPR genes upon ADAR1 depletion during reprogramming (Figure 5A), the hyperactivated ER stress did not lead to increased cell death (Figures S5B and S5C). By analyzing the impact of ADAR1 on the three major stress sensors of the UPR (i.e., ATF6, IRE1α, and PERK) (Figure S5A), we found that ADAR1 catalytic activity loss led to a significant reduction of the activation by phosphorylation of PERK and EIF2α proteins, as well as the protein levels of their downstream target CHOP, the pro-apoptotic transcription factor (Zinszner et al., 1998), without affecting ATF6 or IRE1α UPR branches (Figures 5B and 5C), despite their RNA upregulation (Figure 5A). These results suggest that the ADAR1-dependent RNA A-to-I editing is required for triggering the PERK/EIF2α/CHOP cell death pathway under the condition of chronic ER stress. However, global PERK protein levels are only minimally affected in absence of ADAR1 during MET (1 versus 0.9 in Figure 5D). Instead, we observed that a marked decrease in PERK activation (1 versus 0.3 for pPERK in Figure 5D), which phosphorylates EIF2α (Harding et al., 1999), occurred concomitantly with an increase of the dsRNA sensor MDA5 (1 versus 3.2 in Figure 5D). This led us to speculate that upregulated MDA5 might hinder activation of the UPR-PERK signaling pathway under ADAR1 deficiency. Indeed, loss of *Ifih1* in OSKM-transduced fibroblasts lacking ADAR1 catalytic activity was sufficient to rescue proper activation of the PERK/EIF2α/CHOP UPR branch (Figures 5D, S5D, and S5E).

Collectively, our data establish that RNA editing by ADAR1 is critical for efficient PERK activation, which functionally connects the potential roles of MDA5-mediated dsRNA sensing

Please cite this article in press as: Guallar et al., ADAR1-Dependent RNA Editing Promotes MET and iPSC Reprogramming by Alleviating ER Stress, Cell Stem Cell (2020), https://doi.org/10.1016/j.stem.2020.04.016

CellPress

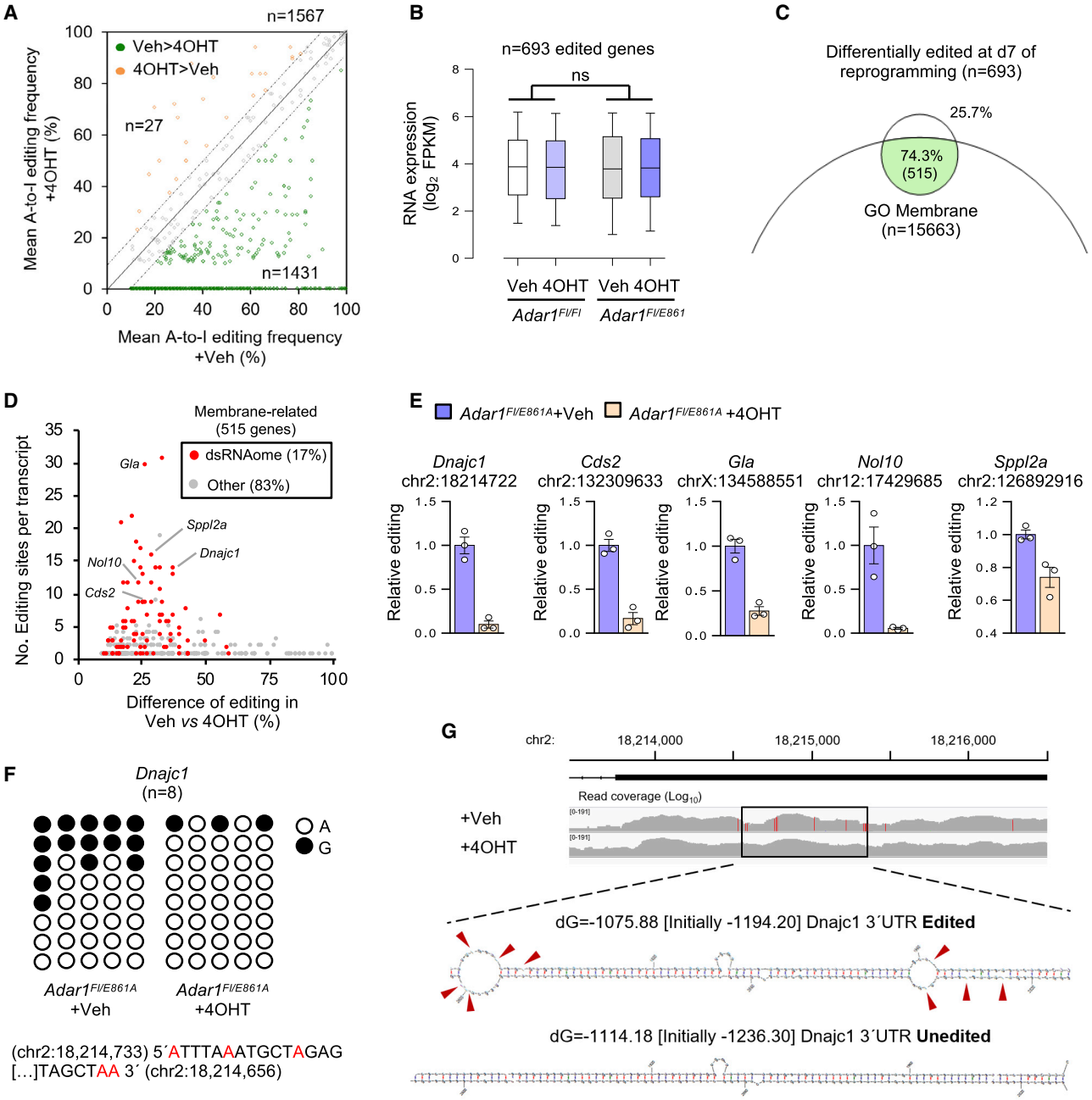

Figure 6. ADAR1 Edits Membrane-Related Transcripts during MET

(A) Scatterplot of A-to-I editing frequency of the 1,567 editing sites detected in WT and heterozygous cells (Veh) in the indicated pooled samples.

(B) Boxplot showing expression (Fragments Per Kilobase Million (FPKM) normalized to the total reads) of ADAR1-dependent edited genes in the indicated cell lines. Whiskers extend to the 10th–90th percentile range. Tukey test for significance was run. ns, not significant.

(C) Overlap of differentially edited transcripts from (A), in the presence or absence of catalytic ADAR1 activity, with genes belonging to membrane-related GOs (GO:0016020, GO:0005783, GO:0031974, GO:0043231, and GO:0043227; see STAR Methods).

(D) Scatterplot of the differentially edited membrane-related RNAs from (C) versus the number of editing sites per transcript. The reported long dsRNAs (Blango and Bass, 2016) are highlighted in red.

(E) Relative abundance of the transcript with the edited site at day 7 of reprogramming of the indicated genotypes. The coordinates of the editing site are indicated below the gene names. Data are shown as mean ± SEM.

(F) Sanger sequencing of *Dnajc1* 3′ UTR RNA in *Adar1* mutant and heterozygous cells at day 7 of reprogramming. Black circles depict inosines, which are sequenced as guanosines.

(legend continued on next page)

Please cite this article in press as: Guallar et al., ADAR1-Dependent RNA Editing Promotes MET and iPSC Reprogramming by Alleviating ER Stress, Cell Stem Cell (2020), https://doi.org/10.1016/j.stem.2020.04.016

with UPR for proper control of IIR/ER stress in reprogramming (Figure S5A, right panel).

ADAR1 Edits Membrane-Related Transcripts during MET

To unravel the underlying mechanism by which ADAR1 modulates MDA5 activity and controls IIR/ER stress during iPSC formation, we aimed to identify dsRNA targets by interrogating ADAR1-specific editing events at the MET time window. We identified 1,431 A-to-I editing sites, corresponding to 693 genes, whose editing frequencies were strongly reduced in absence of ADAR1 catalytic activity (Figures 6A and S6A; Table S2). Most A-to-I sites in coding RNAs were localized to 3′ UTR regions (Figure S6B) without significant impact on transcript abundance (Figure 6B). Notably, whereas only a 3.4% of edited RNA species were mesenchymal- or epithelial-associated genes themselves (Figure S6C), pathway analysis revealed a specific and highly significant association of the differentially edited genes (i.e., 515 from a total of 693 genes) with membrane-related GO terms (Figures 6C and S6D). This is in line with the high percentage of membrane-related genes that are differentially expressed during MET (Figure S6E). In addition, *in silico* prediction revealed that one-third of the 515 differentially edited genes possess ER signal peptides (10%), transmembrane domains (13%), or both (6%), further supporting their association with the ER membrane for translation (Figure S6F). Interestingly, when analyzing these 515 membrane-related genes, we found that an appreciable proportion of them (17%, n = 89 genes) was reported to possess long dsRNA structures (Blango and Bass, 2016) (Figure 6D and S6G), among which are many ER stress-linked genes (Table S3). Of these 89 targets, 28.3% of them were conserved between mouse and human when analyzed with all edited sites available in RADAR database (Ramaswami and Li, 2014) (Figure S6G).

MDA5 was reported to preferentially recognize dsRNA structures that are also ADAR1 targets (Peisley et al., 2012; Walkley and Li, 2017). A-to-I editing has been predicted to induce RNA structural changes (Brümmer et al., 2017; Liddicoat et al., 2015), which could potentially abrogate the formation of perfectly matched long dsRNA leading to the failure in MDA5 sensing (Liddicoat et al., 2015). Accordingly, we validated the presence of A-to-I editing sites in top candidates with dsRNA structures, including the UPR-related heat shock protein DNAJC1 (Figures 6E, 6F, and S6J), by showing that the editing is reduced upon the loss of ADAR1 catalytic activity during MET (Figures 6E, S6H, and S6I). By modeling the secondary structure of *Dnajc1* with the replacement of adenosines with inosines and the assumption of no base-pairing, we observed a higher free energy state resulting from A-to-I substitutions and, consequently, predicted destabilization of perfect dsRNA stem loops (Figure 6G), which could potentially interfere with MDA5 recognition.

Altogether, these results reveal potential targets of ADAR1 whose editing statuses (and thus secondary structures) modulate MDA5 sensing and whose functions are related to membranous organelle ER.

MDA5 Mediates Cytosolic Retention of Unedited Membrane-Related dsRNAs

To understand how those edited membrane-related transcripts, which maintained expression levels regardless of ADAR1 status (Figure 6B), may contribute to ADAR1 functions during reprogramming, we assessed whether A-to-I editing status would alter their proper subcellular localization through MDA5 sensing at the MET stage. We detected that loss of A-to-I editing increased the cytosolic localization of the membrane-related and ADAR1-edited long dsRNAs (Figures 7A, S7A, and S7B). These results indicate that adenosine deamination by ADAR1 restricts the cytosolic distribution of the edited membrane-related dsRNAs during MET. Then, we explored the possibility that MDA5 sensing might interfere with the specific ER compartmentalization of those unedited RNAs. Indeed, several lines of evidence support this to be the case. First, we found that MDA5 was absent in the membrane subcellular fraction and confined to the cytosolic compartment (Figure 7B). Second, we performed immunoprecipitation of MDA5 and confirmed its ability to interact with ADAR1 targets *in vitro* (Figure 7C and 7D). Importantly, we were able to detect ADAR1 targets, including *Dnajc1* and *Cds2*, among MDA5-interacting RNAs, with enhanced *in vitro* binding to MDA5 upon *Adar1* deletion (Figures 7D and S7C). Third, we found that depletion of *Mda5* (i.e., *Ifih1*) in *Adar1* KO or editing mutant cells was sufficient to restore proper RNA subcellular (i.e., membrane-bound) localization during MET (Figures 7E and S7D). However, ectopic expression of several MDA5-sensed RNA candidates individually (i.e., DNAJC1, CDS2, GLA, NOL10, and SPPL2A) was not sufficient to rescue proper UPR function and iPSC generation in ADAR1-depleted cells (Figures S7E and S7F), suggesting a combined action of many of these candidates may mediate ADAR1 functions in reprogramming.

Collectively, these data establish a critical role of MDA5 in mediating cytosolic retention of a subset of ADAR1 targets whose transcripts, when edited, have important ER-related functions (e.g., UPR) to safeguard MET during reprogramming.

DISCUSSION

Our study reveals that ADAR1 acts on the A-to-I RNA editome in promoting transcription-factor-induced reprogramming under multiple cellular contexts with diverse reprogramming cocktails. Mechanistically, ADAR1 prevents MDA5 sensing of a subset of endogenous dsRNA-containing membrane-related RNAs with functional significance in transducing UPR through the PERK pathway for ER homeostasis. Loss of RNA editing by ADAR1 enables MDA5 sensing, which leads to aberrant transcriptional activation of IIR program and hyperactivated ER stress with consequent MET inhibition and compromised iPSC formation (Figure 7F).

(G) Top: Integrative Genomics Viewer image of *Dnajc1* 3′ UTR RNA expression in *Adar1*$^{E1/E861A}$ cells with the indicated treatments. Red lines indicate editing positions. Bottom: secondary structure of the boxed *Dnajc1* 3′ UTR region is shown. The red arrow points indicate the inosine positions. Free energy states of each full 3′ UTR structure are depicted as dG.
See also Figure S6 and Tables S2 and S3.

Please cite this article in press as: Guallar et al., ADAR1-Dependent RNA Editing Promotes MET and iPSC Reprogramming by Alleviating ER Stress, Cell Stem Cell (2020), https://doi.org/10.1016/j.stem.2020.04.016

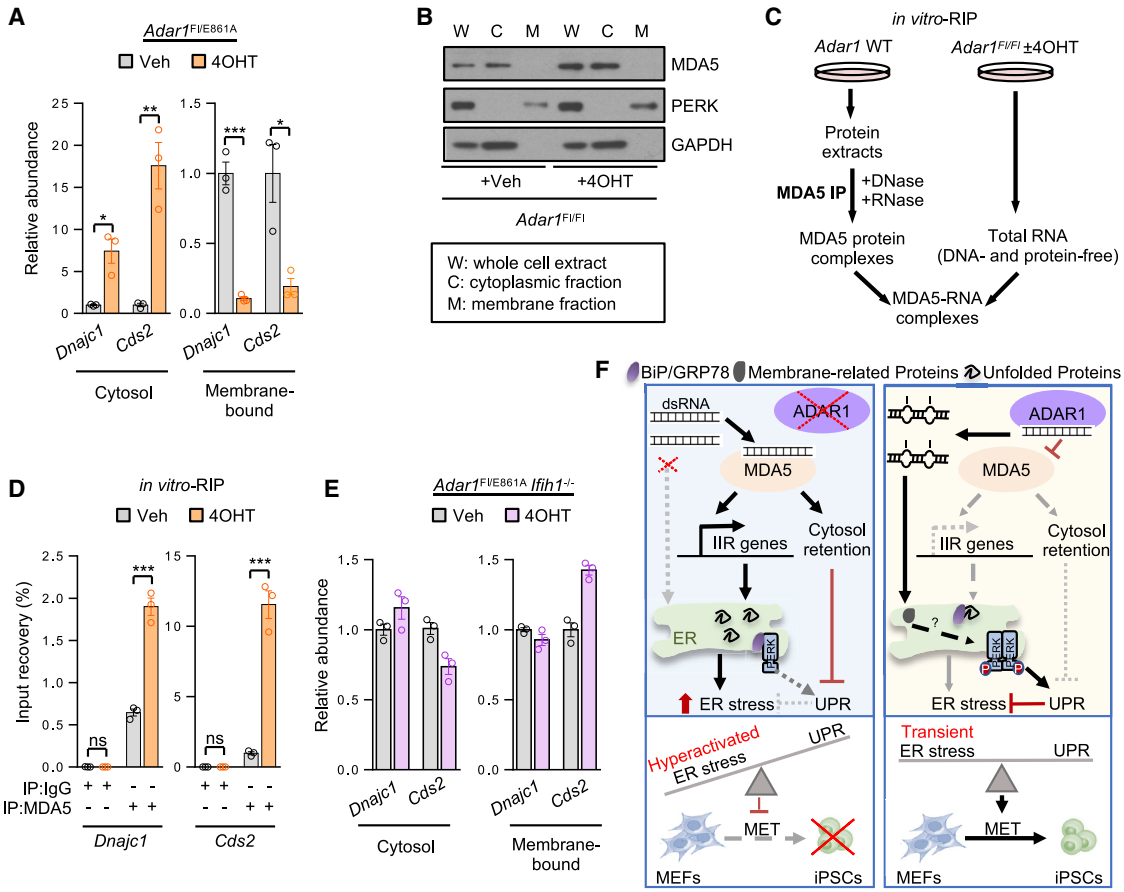

Figure 7. MDA5 Mediates Cytosolic Retention of Unedited Membrane-Related dsRNAs

(A) Relative *Dnajc1* and *Cds2* transcript abundance in cells with the indicated genotypes.

(B) Western blot of MDA5 subcellular localization. PERK and GAPDH were used as membrane-bound and cytoplasmic control proteins, respectively.

(C) Scheme of the *in vitro* RNA immunoprecipitation (*iv*-RIP) protocol (Guallar et al., 2018) used in (D).

(D) Analysis of *Dnajc1* and *Cds2* abundance among IgG or MDA5-interacting RNAs analyzed by *iv*-RIP.

(E) Relative *Dnajc1* and *Cds2* transcript abundance in each subcellular fraction at day 7 of reprogramming.

(F) A schematic model of how RNA editing by ADAR1 safeguards MET for efficient reprogramming.

Data in (A), (D), and (E) are shown as mean ± SEM (n = 3 independent experiments). Two-tailed Student's t test was performed. *p < 0.05; **p < 0.01; ***p < 0.001; ns, not significant. See also Figure S7.

IIR and Somatic Cell Reprogramming

Pattern recognition receptors (PRRs), which include membrane-bound PRRs such as Toll-like receptors (TLRs) and cytoplasmic PRRs such as RIG-I-like receptors (RLRs), play a crucial role in the proper function of the innate immune system (Takeuchi and Akira, 2010). Our study reveals that among the two RLRs, RIG-I and MDA5, which are involved in cytosolic RNA recognition and innate immune activation, only MDA5 depletion was able to restore IIR and subsequent iPSC formation in the absence of ADAR1 (Figure 4D). These findings, together with a previous study showing that membrane-bound TLR3-mediated transient activation of the IIR can enhance nuclear reprogramming (Lee et al., 2012b), underline the importance of a tight regulation of innate immunity in the process of iPSC generation. Further studies are needed to better understand the interplay of specific innate immune signaling pathways in promoting (or restricting) somatic cell reprogramming.

ER Stress, UPR, and Somatic Cell Reprogramming

Our study establishes that hyperactivated ER stress upon the loss of ADAR1 editing activity is a major reprogramming barrier. Loss of *Adar1* was also reported to induce ER stress, causing the loss of intestinal stem cells and disrupting intestinal homeostasis (Qiu et al., 2013). Our observation that activation of UPR enhances iPSC formation (Figures 3I, S3E, and S3I) is in line with a recent report (Simic et al., 2019) and suggests the likely acute accumulation of misfolded proteins in the ER associated with the transient ER stress during reprogramming, which is buffered by the UPR (Figure 7F). Whereas previous studies have shown the existence of adaptive UPR to avoid cell death when ER stress is not mitigated (Guan et al., 2017; Woo et al., 2009; Yao et al., 2017), here we identified a distinct response that involves the catalytic activity of ADAR1 for proper activation of the PERK-UPR signaling branch to maintain ER homeostasis in reprogramming. Thus, we reveal a dual role of A-to-I RNA editing by ADAR1 in

Please cite this article in press as: Guallar et al., ADAR1-Dependent RNA Editing Promotes MET and iPSC Reprogramming by Alleviating ER Stress, Cell Stem Cell (2020), https://doi.org/10.1016/j.stem.2020.04.016

both suppressing aberrant innate immune stimulation that causes ER stress and facilitating proper UPR function (Figure 7F, right panel).

ADAR1's Roles in the Crosstalk between MDA5 dsRNA Sensing and ER Functions

Recent studies have reported mRNA shuttling between the ER and the cytosol as an additional mechanism to modulate protein synthesis upon ER stress (Guan et al., 2017; Reid et al., 2014). However, whether RNA modifications play a role in such regulation has not been defined. In this respect, we identify a subset of ADAR1 membrane-related targets with dsRNA structures that are A-to-I edited in order to prevent their binding and cytosolic retention by MDA5. It is likely that among these MDA5-sequestered RNAs, there are molecular players involved in ER homeostasis whose cellular localization is affected by ADAR1-mediated A-to-I editing. However, it remains to be determined which and how many targets are the key effectors of ADAR1 functions in safeguarding MET for reprogramming.

ADAR1 Functions in MET during Somatic Cell Reprogramming

Our study uncovers that ADAR1 is a previously unrecognized player of epithelial cell fate acquisition during reprogramming of mesenchymal somatic cells while being dispensable for the maintenance of pluripotent epithelial-like cells, as reported previously (Chung et al., 2018; Osenberg et al., 2010). Taking into consideration that ER stress was previously reported to promote mesenchymal cell identity (Tanjore et al., 2011; Zhong et al., 2011), more studies will be required to understand how loss of A-to-I editing would favor mesenchymal cell identity at the expense of epithelial cell fate acquisition during reprogramming. While a previous study reported that accumulated levels of c-JUN and c-FOS favor mesenchymal gene expression activation and inhibit reprogramming (Liu et al., 2015), we did not observe an increase of these proteins upon ADAR1 depletion (Figures S3J and S3K). On the other hand, considering important roles of microRNAs (miRNAs) in MET during reprogramming (Bullock et al., 2012; Samavarchi-Tehrani et al., 2010; Wang et al., 2013) and reported ADAR1 functions in miRNA biogenesis and activity (Bahn et al., 2015; Chen et al., 2015b; Correia de Sousa et al., 2019; Kawahara et al., 2007; Ota et al., 2013; Qi et al., 2017; Vesely et al., 2012; Yang et al., 2006; Zipeto et al., 2016), future studies are warranted to investigate the potential connection between ADAR1 and miRNA pathways in regulating early cell fate decisions during somatic cell reprogramming.

Finally, transitions between MET and its reverse process, epithelial-to-mesenchymal transition (EMT), are key events during development, tissue repair, and tumor progression and dissemination (Lu and Kang, 2019; Polyak and Weinberg, 2009; Thiery et al., 2009). In this regard, it is worth pointing out that both ER stress and ADAR1 have been connected to cancer immunotherapy (Cubillos-Ruiz et al., 2017; Ishizuka et al., 2019) and that there also exists a positive correlation between ADAR1 and EMT in oral squamous cell carcinoma (Liu et al., 2019). In addition, a previous study reported a correlation between loss of function of ADAR1 during human iPSC reprogramming with the appearance of cells with cancer-related properties (Germanguz et al., 2014). Therefore, the crosstalk between ADAR1 catalytic activity and ER stress for MET regulation, discovered in this study, may also have functional implications in cellular reprogramming under a pathological context.

STAR★METHODS

Detailed methods are provided in the online version of this paper and include the following:

- KEY RESOURCES TABLE
- RESOURCE AVAILABILITY
  - Lead Contact
  - Materials Availability
  - Data and Code Availability
- EXPERIMENTAL MODEL AND SUBJECT DETAILS
  - Mice
  - Cells
- METHOD DETAILS
  - shRNA Design and pMX-Based Retroviral Constructs
  - Viral Production
  - OSKM Reprogramming Assays in Somatic Cells to Form iPSCs
  - 7 Factor Reprogramming Assays in Fibroblasts to Form iPSCs
  - Reprogramming Assays Using Reprogramming Intermediates
  - Direct Reprogramming to Neurons
  - iPSC Differentiation Assays
  - Determination of Cell Death
  - Treatment with Endoplasmic Reticulum Stress Inducers and Inhibitors
  - Western Blot Analysis and Quantification
  - Immunofluorescence
  - Alkaline Phosphatase (AP) Staining
  - Colony Formation Assay
  - RNA Extraction and Analysis by Quantitative PCR (RT-qPCR)
  - Analysis of Membrane and Cytoplasmic Fractions
  - *In Vitro* RNA Immunoprecipitation (iv-RIP)
  - RNA Sequencing (RNA-seq) and Analysis
  - Gene Set Enrichment Analysis (GSEA)
  - RNA Editing Detection from Mouse RNA-seq Data
  - Comparison of Editing Levels in MEF and iPSC Samples
  - Principal Component Analysis (PCA) and Gene Ontology (GO)
  - Validation of A-to-I Editing by RT-qPCR
  - Validation of Editing by Sanger Sequencing
  - Editing Analysis Using a Reporter System
  - RNA Secondary Structure Prediction
  - Transmembrane Domains and ER Signal Peptides Prediction
- QUANTIFICATION AND STATISTICAL ANALYSIS

SUPPLEMENTAL INFORMATION

Supplemental Information can be found online at https://doi.org/10.1016/j.stem.2020.04.016.

ACKNOWLEDGMENTS

We thank M. Jantsch for the A-to-I RNA editing reporter constructs and M. Wernig (*Ascl1*) and D. Pei (7F cocktail) for overexpressing constructs. This research was funded by grants from the Spanish Agencia Estatal de Investigación, co-funded by the FEDER Program of the EU (BFU2016-80899-P to M.F. and RTI2018-096708-J-I00 to D.G.) (AEI/FEDER, UE); the Xunta de Galicia-Consellería de Cultura, Educación e Ordenación Universitaria (ED431F 2016/016 to M.F.); the Fundación Ramón Areces (2016-PO025 to M.F.); the New York State Department of Health (C32583GG and C32569GG to J.W.); and the National Institutes of Health (NIH) (GM129157, HD095938, and HD097268 to J.W.). Research from the C.R.W. laboratory was supported by the National Health and Medical Research Council (NHMRC) (APP1102006/APP1144049), the Australian Research Council (DP180103989), and a Victorian Cancer Agency research fellowship (MCRF15015). Research from the M.L. laboratory was supported by Xunta de Galicia (2016-PG068) and Ministerio de Economía y Competitividad (MINECO), co-funded by the FEDER Program of the EU (RTI2018-101840-B-I00) and Atresmedia. L.J.L. was funded by the Guangzhou Health-Medical Collaborative Innovation Project (201400000004-5). M.F. and M.G.B. are recipients of Ramón y Cajal awards (RYC-2014-16779 to M.F. and RYC-2012-10835 to M.G.B.) from the MINECO of Spain, and J.W. is a recipient of an Irma T. Hirschl and Weill-Caulier Trusts Career Scientist Award. A.F.-I. (MINECO, BES-2017-082007), Y.S. (Xunta de Galicia, ED481A-2017/166), and A.E. and V.G.-O. (Ministerio de Ciencia, Innovación y Universidades, FPU2018/01246 and FPU17/01131, respectively) are recipients of fellowships. CIBER de Fisiopatología de la Obesidad y Nutrición is an initiative of ISCIII.

AUTHOR CONTRIBUTIONS

D.G. and A.F.-I. conducted the experiments, and A.F.-I. performed the computational analysis. H.X., D.L., S.X., Y.H., K.W., and L.J.L. developed a mouse-specific A-to-I editing pipeline and performed computational analysis. Y.S., C.A., O.F.-A., J.A.P., A.E., V.G.-O., T.M., C.S., D.T., J.C.H., M.G.B., M.L., and C.R.W. provided reagents and performed experiments. D.G., J.W., and M.F. wrote the manuscript with contributions from all other authors. D.G., J.W., and M.F. conceived, designed, and supervised the studies and approved the final manuscript.

DECLARATION OF INTERESTS

The authors declare no competing interests.

Received: August 22, 2019
Revised: April 2, 2020
Accepted: April 23, 2020
Published: May 11, 2020

REFERENCES

Aguilo, F., Zhang, F., Sancho, A., Fidalgo, M., Di Cecilia, S., Vashisht, A., Lee, D.F., Chen, C.H., Rengasamy, M., Andino, B., et al. (2015). Coordination of m(6)A mRNA Methylation and Gene Transcription by ZFP217 Regulates Pluripotency and Reprogramming. Cell Stem Cell *17*, 689–704.

Apostolou, E., and Stadtfeld, M. (2018). Cellular trajectories and molecular mechanisms of iPSC reprogramming. Curr. Opin. Genet. Dev. *52*, 77–85.

Bahn, J.H., Ahn, J., Lin, X., Zhang, Q., Lee, J.H., Civelek, M., and Xiao, X. (2015). Genomic analysis of ADAR1 binding and its involvement in multiple RNA processing pathways. Nat. Commun. *6*, 6355.

Bettigole, S.E., and Glimcher, L.H. (2015). Endoplasmic reticulum stress in immunity. Annu. Rev. Immunol. *33*, 107–138.

Blango, M.G., and Bass, B.L. (2016). Identification of the long, edited dsRNAome of LPS-stimulated immune cells. Genome Res. *26*, 852–862.

Boyce, M., Bryant, K.F., Jousse, C., Long, K., Harding, H.P., Scheuner, D., Kaufman, R.J., Ma, D., Coen, D.M., Ron, D., and Yuan, J. (2005). A selective inhibitor of eIF2alpha dephosphorylation protects cells from ER stress. Science *307*, 935–939.

Brümmer, A., Yang, Y., Chan, T.W., and Xiao, X. (2017). Structure-mediated modulation of mRNA abundance by A-to-I editing. Nat. Commun. *8*, 1255.

Bullock, M.D., Sayan, A.E., Packham, G.K., and Mirnezami, A.H. (2012). MicroRNAs: critical regulators of epithelial to mesenchymal (EMT) and mesenchymal to epithelial transition (MET) in cancer progression. Biol. Cell *104*, 3–12.

Chanda, S., Ang, C.E., Davila, J., Pak, C., Mall, M., Lee, Q.Y., Ahlenius, H., Jung, S.W., Südhof, T.C., and Wernig, M. (2014). Generation of induced neuronal cells by the single reprogramming factor ASCL1. Stem Cell Reports *3*, 282–296.

Chen, C.X., Cho, D.S., Wang, Q., Lai, F., Carter, K.C., and Nishikura, K. (2000). A third member of the RNA-specific adenosine deaminase gene family, ADAR3, contains both single- and double-stranded RNA binding domains. RNA *6*, 755–767.

Chen, T., Hao, Y.J., Zhang, Y., Li, M.M., Wang, M., Han, W., Wu, Y., Lv, Y., Hao, J., Wang, L., et al. (2015a). m(6)A RNA methylation is regulated by microRNAs and promotes reprogramming to pluripotency. Cell Stem Cell *16*, 289–301.

Chen, T., Xiang, J.F., Zhu, S., Chen, S., Yin, Q.F., Zhang, X.O., Zhang, J., Feng, H., Dong, R., Li, X.J., et al. (2015b). ADAR1 is required for differentiation and neural induction by regulating microRNA processing in a catalytically independent manner. Cell Res. *25*, 459–476.

Chung, H., Calis, J.J.A., Wu, X., Sun, T., Yu, Y., Sarbanes, S.L., Dao Thi, V.L., Shilvock, A.R., Hoffmann, H.H., Rosenberg, B.R., et al. (2018). Human ADAR1 prevents endogenous RNA from triggering translational shutdown. Cell *172*, 811–824.e814.

Contreras, C., González-García, I., Martínez-Sánchez, N., Seoane-Collazo, P., Jacas, J., Morgan, D.A., Serra, D., Gallego, R., Gonzalez, F., Casals, N., et al. (2014). Central ceramide-induced hypothalamic lipotoxicity and ER stress regulate energy balance. Cell Rep. *9*, 366–377.

Correia de Sousa, M., Gjorgjieva, M., Dolicka, D., Sobolewski, C., and Foti, M. (2019). Deciphering miRNAs' action through miRNA editing. Int. J. Mol. Sci. *20*, E6249.

Costa, Y., Ding, J., Theunissen, T.W., Faiola, F., Hore, T.A., Shliaha, P.V., Fidalgo, M., Saunders, A., Lawrence, M., Dietmann, S., et al. (2013). NANOG-dependent function of TET1 and TET2 in establishment of pluripotency. Nature *495*, 370–374.

Cubillos-Ruiz, J.R., Bettigole, S.E., and Glimcher, L.H. (2017). Tumorigenic and immunosuppressive effects of endoplasmic reticulum stress in cancer. Cell *168*, 692–706.

Diehn, M., Eisen, M.B., Botstein, D., and Brown, P.O. (2000). Large-scale identification of secreted and membrane-associated gene products using DNA microarrays. Nat. Genet. *25*, 58–62.

Doetschman, T.C., Eistetter, H., Katz, M., Schmidt, W., and Kemler, R. (1985). The in vitro development of blastocyst-derived embryonic stem cell lines: formation of visceral yolk sac, blood islands and myocardium. J. Embryol. Exp. Morphol. *87*, 27–45.

Eminli, S., Foudi, A., Stadtfeld, M., Maherali, N., Ahfeldt, T., Mostoslavsky, G., Hock, H., and Hochedlinger, K. (2009). Differentiation stage determines potential of hematopoietic cells for reprogramming into induced pluripotent stem cells. Nat. Genet. *41*, 968–976.

Frye, M., Harada, B.T., Behm, M., and He, C. (2018). RNA modifications modulate gene expression during development. Science *361*, 1346–1349.

Fu, S., Yalcin, A., Lee, G.Y., Li, P., Fan, J., Arruda, A.P., Pers, B.M., Yilmaz, M., Eguchi, K., and Hotamisligil, G.S. (2015). Phenotypic assays identify azoramide as a small-molecule modulator of the unfolded protein response with antidiabetic activity. Sci. Transl. Med. *7*, 292ra98.

Germanguz, I., Shtrichman, R., Osenberg, S., Ziskind, A., Novak, A., Domev, H., Laevsky, I., Jacob-Hirsch, J., Feiler, Y., Rechavi, G., and Itskovitz-Eldor, J. (2014). ADAR1 is involved in the regulation of reprogramming human fibroblasts to induced pluripotent stem cells. Stem Cells Dev. *23*, 443–456.

Guallar, D., Bi, X., Pardavila, J.A., Huang, X., Saenz, C., Shi, X., Zhou, H., Faiola, F., Ding, J., Haruehanroengra, P., et al. (2018). RNA-dependent chromatin targeting of TET2 for endogenous retrovirus control in pluripotent stem cells. Nat. Genet. *50*, 443–451.

Guan, B.J., van Hoef, V., Jobava, R., Elroy-Stein, O., Valasek, L.S., Cargnello, M., Gao, X.H., Krokowski, D., Merrick, W.C., Kimball, S.R., et al. (2017). A unique ISR program determines cellular responses to chronic stress. Mol. Cell *68*, 885–900 e886.

Hansson, J., Rafiee, M.R., Reiland, S., Polo, J.M., Gehring, J., Okawa, S., Huber, W., Hochedlinger, K., and Krijgsveld, J. (2012). Highly coordinated proteome dynamics during reprogramming of somatic cells to pluripotency. Cell Rep. *2*, 1579–1592.

Harding, H.P., Zhang, Y., and Ron, D. (1999). Protein translation and folding are coupled by an endoplasmic-reticulum-resident kinase. Nature *397*, 271–274.

Haridhasapavalan, K.K., Raina, K., Dey, C., Adhikari, P., and Thummer, R.P. (2020). An Insight into reprogramming barriers to iPSC generation. Stem Cell Rev. Rep. *16*, 56–81.

Hartner, J.C., Walkley, C.R., Lu, J., and Orkin, S.H. (2009). ADAR1 is essential for the maintenance of hematopoiesis and suppression of interferon signaling. Nat. Immunol. *10*, 109–115.

Hendershot, L.M., Wei, J.Y., Gaut, J.R., Lawson, B., Freiden, P.J., and Murti, K.G. (1995). In vivo expression of mammalian BiP ATPase mutants causes disruption of the endoplasmic reticulum. Mol. Biol. Cell *6*, 283–296.

Heraud-Farlow, J.E., Chalk, A.M., Linder, S.E., Li, Q., Taylor, S., White, J.M., Pang, L., Liddicoat, B.J., Gupte, A., Li, J.B., and Walkley, C.R. (2017). Protein recoding by ADAR1-mediated RNA editing is not essential for normal development and homeostasis. Genome Biol. *18*, 166.

Hetz, C. (2012). The unfolded protein response: controlling cell fate decisions under ER stress and beyond. Nat. Rev. Mol. Cell Biol. *13*, 89–102.

Huang da, W., Sherman, B.T., and Lempicki, R.A. (2009). Bioinformatics enrichment tools: paths toward the comprehensive functional analysis of large gene lists. Nucleic Acids Res. *37*, 1–13.

Ishizuka, J.J., Manguso, R.T., Cheruiyot, C.K., Bi, K., Panda, A., Iracheta-Vellve, A., Miller, B.C., Du, P.P., Yates, K.B., Dubrot, J., et al. (2019). Loss of ADAR1 in tumours overcomes resistance to immune checkpoint blockade. Nature *565*, 43–48.

Jagannathan, S., Nwosu, C., and Nicchitta, C.V. (2011). Analyzing mRNA localization to the endoplasmic reticulum via cell fractionation. Methods Mol. Biol. *714*, 301–321.

Kawahara, Y., Zinshteyn, B., Sethupathy, P., Iizasa, H., Hatzigeorgiou, A.G., and Nishikura, K. (2007). Redirection of silencing targets by adenosine-to-inosine editing of miRNAs. Science *315*, 1137–1140.

Lamers, M.M., van den Hoogen, B.G., and Haagmans, B.L. (2019). ADAR1: "Editor-in-Chief" of cytoplasmic innate immunity. Front. Immunol. *10*, 1763.

Lee, J., Sayed, N., Hunter, A., Au, K.F., Wong, W.H., Mocarski, E.S., Pera, R.R., Yakubov, E., and Cooke, J.P. (2012b). Activation of innate immunity is required for efficient nuclear reprogramming. Cell *151*, 547–558.

Lee, D.F., Su, J., Sevilla, A., Gingold, J., Schaniel, C., and Lemischka, I.R. (2012a). Combining competition assays with genetic complementation strategies to dissect mouse embryonic stem cell self-renewal and pluripotency. Nat. Protoc. *7*, 729–748.

Li, H., and Durbin, R. (2009). Fast and accurate short read alignment with Burrows-Wheeler transform. Bioinformatics *25*, 1754–1760.

Li, R., Liang, J., Ni, S., Zhou, T., Qing, X., Li, H., He, W., Chen, J., Li, F., Zhuang, Q., et al. (2010). A mesenchymal-to-epithelial transition initiates and is required for the nuclear reprogramming of mouse fibroblasts. Cell Stem Cell *7*, 51–63.

Liddicoat, B.J., Piskol, R., Chalk, A.M., Ramaswami, G., Higuchi, M., Hartner, J.C., Li, J.B., Seeburg, P.H., and Walkley, C.R. (2015). RNA editing by ADAR1 prevents MDA5 sensing of endogenous dsRNA as nonself. Science *349*, 1115–1120.

Liu, X., Fu, Y., Huang, J., Wu, M., Zhang, Z., Xu, R., Zhang, P., Zhao, S., Liu, L., and Jiang, H. (2019). ADAR1 promotes the epithelial-to-mesenchymal transition and stem-like cell phenotype of oral cancer by facilitating oncogenic microRNA maturation. J. Exp. Clin. Cancer Res. *38*, 315.

Liu, J., Han, Q., Peng, T., Peng, M., Wei, B., Li, D., Wang, X., Yu, S., Yang, J., Cao, S., et al. (2015). The oncogene c-Jun impedes somatic cell reprogramming. Nat. Cell Biol. *17*, 856–867.

Lu, W., and Kang, Y. (2019). Epithelial-mesenchymal plasticity in cancer progression and metastasis. Dev. Cell *49*, 361–374.

Mannion, N.M., Greenwood, S.M., Young, R., Cox, S., Brindle, J., Read, D., Nellåker, C., Vesely, C., Ponting, C.P., McLaughlin, P.J., et al. (2014). The RNA-editing enzyme ADAR1 controls innate immune responses to RNA. Cell Rep. *9*, 1482–1494.

Martinez-Sanchez, N., Seoane-Collazo, P., Contreras, C., Varela, L., Villarroya, J., Rial-Pensado, E., Buque, X., Aurrekoetxea, I., Delgado, T.C., Vazquez-Martinez, R., et al. (2017). Hypothalamic AMPK-ER stress-JNK1 axis mediates the central actions of thyroid hormones on energy balance. Cell Metab. *26*, 212–229.e212.

Oakes, E., Anderson, A., Cohen-Gadol, A., and Hundley, H.A. (2017). Adenosine deaminase that acts on RNA 3 (ADAR3) binding to glutamate receptor subunit B pre-mRNA inhibits RNA editing in glioblastoma. J. Biol. Chem. *292*, 4326–4335.

Osenberg, S., Paz Yaacov, N., Safran, M., Moshkovitz, S., Shtrichman, R., Sherf, O., Jacob-Hirsch, J., Keshet, G., Amariglio, N., Itskovitz-Eldor, J., and Rechavi, G. (2010). Alu sequences in undifferentiated human embryonic stem cells display high levels of A-to-I RNA editing. PLoS ONE *5*, e11173.

Ota, H., Sakurai, M., Gupta, R., Valente, L., Wulff, B.E., Ariyoshi, K., Iizasa, H., Davuluri, R.V., and Nishikura, K. (2013). ADAR1 forms a complex with Dicer to promote microRNA processing and RNA-induced gene silencing. Cell *153*, 575–589.

Peisley, A., Jo, M.H., Lin, C., Wu, B., Orme-Johnson, M., Walz, T., Hohng, S., and Hur, S. (2012). Kinetic mechanism for viral dsRNA length discrimination by MDA5 filaments. Proc. Natl. Acad. Sci. USA *109*, E3340–E3349.

Pestal, K., Funk, C.C., Snyder, J.M., Price, N.D., Treuting, P.M., and Stetson, D.B. (2015). Isoforms of RNA-editing enzyme ADAR1 independently control nucleic acid sensor MDA5-driven autoimmunity and multi-organ development. Immunity *43*, 933–944.

Plath, K., and Lowry, W.E. (2011). Progress in understanding reprogramming to the induced pluripotent state. Nat. Rev. Genet. *12*, 253–265.

Polyak, K., and Weinberg, R.A. (2009). Transitions between epithelial and mesenchymal states: acquisition of malignant and stem cell traits. Nat. Rev. Cancer *9*, 265–273.

Qi, L., Song, Y., Chan, T.H.M., Yang, H., Lin, C.H., Tay, D.J.T., Hong, H., Tang, S.J., Tan, K.T., Huang, X.X., et al. (2017). An RNA editing/dsRNA binding-independent gene regulatory mechanism of ADARs and its clinical implication in cancer. Nucleic Acids Res. *45*, 10436–10451.

Qiu, W., Wang, X., Buchanan, M., He, K., Sharma, R., Zhang, L., Wang, Q., and Yu, J. (2013). ADAR1 is essential for intestinal homeostasis and stem cell maintenance. Cell Death Dis. *4*, e599.

Ramaswami, G., and Li, J.B. (2014). RADAR: a rigorously annotated database of A-to-I RNA editing. Nucleic Acids Res. *42*, D109–D113.

Ramaswami, G., Lin, W., Piskol, R., Tan, M.H., Davis, C., and Li, J.B. (2012). Accurate identification of human Alu and non-Alu RNA editing sites. Nat. Methods *9*, 579–581.

Reid, D.W., Chen, Q., Tay, A.S., Shenolikar, S., and Nicchitta, C.V. (2014). The unfolded protein response triggers selective mRNA release from the endoplasmic reticulum. Cell *158*, 1362–1374.

Reid, D.W., and Nicchitta, C.V. (2012). Primary role for endoplasmic reticulum-bound ribosomes in cellular translation identified by ribosome profiling. J. Biol. Chem. *287*, 5518–5527.

Rice, G.I., Kasher, P.R., Forte, G.M., Mannion, N.M., Greenwood, S.M., Szynkiewicz, M., Dickerson, J.E., Bhaskar, S.S., Zampini, M., Briggs, T.A., et al. (2012). Mutations in ADAR1 cause Aicardi-Goutières syndrome associated with a type I interferon signature. Nat. Genet. *44*, 1243–1248.

Rice, G.I., Kitabayashi, N., Barth, M., Briggs, T.A., Burton, A.C.E., Carpanelli, M.L., Cerisola, A.M., Colson, C., Dale, R.C., Danti, F.R., et al. (2017). Genetic, phenotypic, and interferon biomarker status in ADAR1-related neurological disease. Neuropediatrics *48*, 166–184.

Roundtree, I.A., Evans, M.E., Pan, T., and He, C. (2017). Dynamic RNA modifications in gene expression regulation. Cell *169*, 1187–1200.

Samavarchi-Tehrani, P., Golipour, A., David, L., Sung, H.K., Beyer, T.A., Datti, A., Woltjen, K., Nagy, A., and Wrana, J.L. (2010). Functional genomics reveals a BMP-driven mesenchymal-to-epithelial transition in the initiation of somatic cell reprogramming. Cell Stem Cell *7*, 64–77.

Schröder, M., and Kaufman, R.J. (2005). The mammalian unfolded protein response. Annu. Rev. Biochem. *74*, 739–789.

Simic, M.S., Moehle, E.A., Schinzel, R.T., Lorbeer, F.K., Halloran, J.J., Heydari, K., Sanchez, M., Jullie, D., Hockemeyer, D., and Dillin, A. (2019). Transient activation of the UPR(ER) is an essential step in the acquisition of pluripotency during reprogramming. Sci. Adv. *5*, eaaw0025.

So, J.S. (2018). Roles of endoplasmic reticulum stress in immune responses. Mol. Cells *41*, 705–716.

Staerk, J., Dawlaty, M.M., Gao, Q., Maetzel, D., Hanna, J., Sommer, C.A., Mostoslavsky, G., and Jaenisch, R. (2010). Reprogramming of human peripheral blood cells to induced pluripotent stem cells. Cell Stem Cell *7*, 20–24.

Takahashi, K., Tanabe, K., Ohnuki, M., Narita, M., Ichisaka, T., Tomoda, K., and Yamanaka, S. (2007). Induction of pluripotent stem cells from adult human fibroblasts by defined factors. Cell *131*, 861–872.

Takahashi, K., and Yamanaka, S. (2006). Induction of pluripotent stem cells from mouse embryonic and adult fibroblast cultures by defined factors. Cell *126*, 663–676.

Takeuchi, O., and Akira, S. (2010). Pattern recognition receptors and inflammation. Cell *140*, 805–820.

Tanjore, H., Cheng, D.S., Degryse, A.L., Zoz, D.F., Abdolrasulnia, R., Lawson, W.E., and Blackwell, T.S. (2011). Alveolar epithelial cells undergo epithelial-to-mesenchymal transition in response to endoplasmic reticulum stress. J. Biol. Chem. *286*, 30972–30980.

Tariq, A., Garncarz, W., Handl, C., Balik, A., Pusch, O., and Jantsch, M.F. (2013). RNA-interacting proteins act as site-specific repressors of ADAR2-mediated RNA editing and fluctuate upon neuronal stimulation. Nucleic Acids Res. *41*, 2581–2593.

Thiery, J.P., Acloque, H., Huang, R.Y., and Nieto, M.A. (2009). Epithelial-mesenchymal transitions in development and disease. Cell *139*, 871–890.

Thomson, M., Liu, S.J., Zou, L.N., Smith, Z., Meissner, A., and Ramanathan, S. (2011). Pluripotency factors in embryonic stem cells regulate differentiation into germ layers. Cell *145*, 875–889.

Vesely, C., Tauber, S., Sedlazeck, F.J., von Haeseler, A., and Jantsch, M.F. (2012). Adenosine deaminases that act on RNA induce reproducible changes in abundance and sequence of embryonic miRNAs. Genome Res. *22*, 1468–1476.

Vierbuchen, T., Ostermeier, A., Pang, Z.P., Kokubu, Y., Südhof, T.C., and Wernig, M. (2010). Direct conversion of fibroblasts to functional neurons by defined factors. Nature *463*, 1035–1041.

Walkley, C.R., and Li, J.B. (2017). Rewriting the transcriptome: adenosine-to-inosine RNA editing by ADARs. Genome Biol. *18*, 205.

Wang, G., Guo, X., Hong, W., Liu, Q., Wei, T., Lu, C., Gao, L., Ye, D., Zhou, Y., Chen, J., et al. (2013). Critical regulation of miR-200/ZEB2 pathway in Oct4/Sox2-induced mesenchymal-to-epithelial transition and induced pluripotent stem cell generation. Proc. Natl. Acad. Sci. USA *110*, 2858–2863.

Wang, M., and Kaufman, R.J. (2016). Protein misfolding in the endoplasmic reticulum as a conduit to human disease. Nature *529*, 326–335.

Wang, Z., Lian, J., Li, Q., Zhang, P., Zhou, Y., Zhan, X., and Zhang, G. (2016). RES-Scanner: a software package for genome-wide identification of RNA-editing sites. Gigascience *5*, 37.

Wang, B., Wu, L., Li, D., Liu, Y., Guo, J., Li, C., Yao, Y., Wang, Y., Zhao, G., Wang, X., et al. (2019). Induction of pluripotent stem cells from mouse embryonic fibroblasts by Jdp2-Jhdm1b-Mkk6-Glis1-Nanog-Essrb-Sall4. Cell Rep. *27*, 3473–3485.e3475.

Woo, C.W., Cui, D., Arellano, J., Dorweiler, B., Harding, H., Fitzgerald, K.A., Ron, D., and Tabas, I. (2009). Adaptive suppression of the ATF4-CHOP branch of the unfolded protein response by toll-like receptor signalling. Nat. Cell Biol. *11*, 1473–1480.

Xiong, H., Liu, D., Li, Q., Lei, M., Xu, L., Wu, L., Wang, Z., Ren, S., Li, W., Xia, M., et al. (2017). RED-ML: a novel, effective RNA editing detection method based on machine learning. Gigascience *6*, 1–8.

Yang, W., Chendrimada, T.P., Wang, Q., Higuchi, M., Seeburg, P.H., Shiekhattar, R., and Nishikura, K. (2006). Modulation of microRNA processing and expression through RNA editing by ADAR deaminases. Nat. Struct. Mol. Biol. *13*, 13–21.

Yao, Y., Lu, Q., Hu, Z., Yu, Y., Chen, Q., and Wang, Q.K. (2017). A non-canonical pathway regulates ER stress signaling and blocks ER stress-induced apoptosis and heart failure. Nat. Commun. *8*, 133.

Ye, S., Dhillon, S., Ke, X., Collins, A.R., and Day, I.N. (2001). An efficient procedure for genotyping single nucleotide polymorphisms. Nucleic Acids Res. *29*, E88–E8.

Zhong, Q., Zhou, B., Ann, D.K., Minoo, P., Liu, Y., Banfalvi, A., Krishnaveni, M.S., Dubourd, M., Demaio, L., Willis, B.C., et al. (2011). Role of endoplasmic reticulum stress in epithelial-mesenchymal transition of alveolar epithelial cells: effects of misfolded surfactant protein. Am. J. Respir. Cell Mol. Biol. *45*, 498–509.

Zinszner, H., Kuroda, M., Wang, X., Batchvarova, N., Lightfoot, R.T., Remotti, H., Stevens, J.L., and Ron, D. (1998). CHOP is implicated in programmed cell death in response to impaired function of the endoplasmic reticulum. Genes Dev. *12*, 982–995.

Zipeto, M.A., Court, A.C., Sadarangani, A., Delos Santos, N.P., Balaian, L., Chun, H.J., Pineda, G., Morris, S.R., Mason, C.N., Geron, I., et al. (2016). ADAR1 activation drives leukemia stem cell self-renewal by impairing Let-7 biogenesis. Cell Stem Cell *19*, 177–191.

Li, H., Handsaker, B., Wysoker, A., Fennell, T., Ruan, J., Homer, N., Marth, G., Abecasis, G., and Durbin, R.; 1000 Genome Project Data Processing Subgroup (2009). The Sequence Alignment/Map format and SAMtools. Bioinformatics *25*, 2078–2079.

Please cite this article in press as: Guallar et al., ADAR1-Dependent RNA Editing Promotes MET and iPSC Reprogramming by Alleviating ER Stress, Cell Stem Cell (2020), https://doi.org/10.1016/j.stem.2020.04.016

STAR★METHODS

KEY RESOURCES TABLE

REAGENT or RESOURCE	SOURCE	IDENTIFIER
Antibodies		
Alexa488-conjugated donkey anti-mouse IgG	Jackson ImmunoResearch	Cat# 711-545-150; RRID:AB_2340846
DyLight 488 conjugate mouse monoclonal SSEA1	ThermoFisher Scientific	Cat# MA1-022-D488; RRID: AB_2536694
Mouse IgG	Sigma-Aldrich	Cat# 12-371; RRID:AB_145840
Mouse monoclonal ACTB	Santa Cruz Biotechnology	Cat# sc-47778; RRID:AB_626632
Mouse monoclonal CDH1	BD Biosciences	Cat# 610182; RRID:AB_397581
Mouse monoclonal CDH2	Santa Cruz Biotechnology	Cat# sc-393933; RRID:AB_2832921
Mouse monoclonal NANOG	Bethyl Laboratories	Cat# A300-397A; RRID:AB_386108
Mouse monoclonal NANOG (human NANOG staining)	Santa Cruz Biotechnology	Cat# sc-374103; RRID:AB_10918255
Mouse monoclonal β-TUBULIN	Santa Cruz Biotechnology	Cat#sc-55529; RRID:AB_2210962
Rabbit monoclonal PERK	Cell Signaling	Cat# 3192; RRID:AB_2095847
Rabbit monoclonal phospho-PERK (Thr980)	Cell Signaling	Cat# 3179; RRID:AB_2095853
Rabbit polyclonal ATF6α	Santa Cruz Biotechnology	Cat# sc-22799; RRID:AB_2242950
Rabbit polyclonal CHOP	Santa Cruz Biotechnology	Cat# sc-793; RRID:AB_631364
Rabbit polyclonal MDA5	Proteintech	Cat# 21775-1-AP; RRID:AB_10734593
Rabbit polyclonal phospho-EIF2α (Ser52)	Santa Cruz Biotechnology	Cat# sc-101670; RRID:AB_2096507
Rabbit polyclonal phospho-IRE (S724)	Abcam	Cat# ab48187; RRID:AB_873899
Mouse monoclonal TUJ1	GeneTex	Cat# GTX631836; RRID:AB_2814952
Rabbit polyclonal c-FOS	Santa Cruz Biotechnology	Cat# sc-166940; RRID:AB_10609634
Mouse monoclonal c-JUN	Santa Cruz Biotechnology	Cat# sc-74543; RRID:AB_1121646
Bacterial and Virus Strains		
Stbl3	This laboratory	N/A
Adenoviral GRP78	Viraquest	N/A
Adenoviral GRP78-DN	Viraquest	N/A
Chemicals, Peptides, and Recombinant Proteins		
CHIR99021	Sigma-Aldrich	Cat# SML1046
PD0325901	Sigma-Aldrich	Cat# PZ0162
bFGF	GIBCO	Cat# PHG0026
BMP4	GIBCO	Cat# PHC9534
Dulbecco's modified Eagle's Medium	Corning	Cat# 10-013-CVR
Dulbecco's Modified Eagle's Medium/Nutrient Mixture F-12 Ham	Sigma-Aldrich	Cat# D6421
RPMI 1640 Medium	Sigma-Aldrich	Cat# R0883
KnockOut Serum Replacement Medium	GIBCO	Cat# 10828028
Neurobasal Medium	GIBCO	Cat# 21103049
Fetal bovine serum	GIBCO	Cat# 10270-106
B-27 Supplement	GIBCO	Cat# 17504-044
N-2 Supplement	GIBCO	Cat# 17502-048
L-Glutamine	GE Healthcare	Cat# SH30034.01
Adenosine	Sigma-Aldrich	Cat# A4036
Cytidine	Sigma-Aldrich	Cat# C4654
Thymidine	Sigma-Aldrich	Cat# T1895
Guanosine	Sigma-Aldrich	Cat# G6264
Sodium pyruvate	Sigma-Aldrich	Cat# S8636

(*Continued on next page*)

Please cite this article in press as: Guallar et al., ADAR1-Dependent RNA Editing Promotes MET and iPSC Reprogramming by Alleviating ER Stress, Cell Stem Cell (2020), https://doi.org/10.1016/j.stem.2020.04.016

Continued

REAGENT or RESOURCE	SOURCE	IDENTIFIER
Non-essential amino acids	GIBCO	Cat# 11140
2-mercaptoethanol	Sigma Aldrich	Cat# M6250
Insulin	Sigma-Aldrich	Cat# I2643
Penicillin and streptomycin	GIBCO	Cat# 15140
Puromycin	Fisher Bioreagents	Cat# BP2956-100
G-418	Corning	Cat# 15303681
Hygromycin	Corning	Cat# 30-240-R
Staurosporine	Sigma-Aldrich	Cat# S5921
Lipofectamine 3000 Reagent	Invitrogen	Cat# L3000-015
Polyethylenimine	Sigma-Aldrich	Cat# 408727
4-hydroxytamoxifen	Sigma-Aldrich	Cat# H7904
Doxycycline	Sigma-Aldrich	Cat# D9891
Azoramide	Cayman	Cat# 18045
Salubrinal	Cayman	Cat# 14735
Thapsigargin	Tocris	Cat# 1138
Tunicamycin	Sigma-Aldrich	Cat# T7765
Protease Inhibitor Cocktail	Sigma-Aldrich	Cat# P8340
Proteinase K	ThermoFisher Scientific	Cat# EO0491
DNase I	ThermoFisher Scientific	EN0521
RNase OUT	Invitrogen	Cat# 10777019
Benzonase nuclease	Sigma-Aldrich	Cat# E1014-5KU
TRIzol	Invitrogen	Cat# 15596026
Critical Commercial Assays		
Alkaline Phosphatase (AP) Staining	Sigma-Aldrich	Cat# 86R-1KT
Amicon Ultra-15 Centrifugal Filters	Amicon	Cat# UFC903024
CloneJet PCR Cloning kit	ThermoFisher Scientific	Cat# K1231
Direct-zol RNA Miniprep Plus Kit	Zymo Research	Cat# R2070
Dynabeads Protein G	Invitrogen	Cat# 10004D
E.Z.N.A Total RNA Kit I	Omega	Cat# R6834-02
Fast SYBR® Green Master Mix	Applied Biosystems	Cat# A25742
T4 DNA Ligase	ThermoFisher Scientific	Cat# EL0016
GenElute Gel Extraction Kit	Sigma-Aldrich	Cat# NA1111
GenElute Plasmid Miniprep Kit	Sigma-Aldrich	Cat# PLN350
jetPRIME Transfection Reagent	Polyplus	Cat#114-01
NEBNext Magnesium RNA Fragmentation Module	NEB	Cat# 6186A
Novex WedgeWell 4-20% Trsi-Glycine Gels	Invitrogen	Cat# XP04205BOX
Phasemaker tubes	Invitrogen	Cat# 15642268
qSCRIPT	Quanta	Cat#84034
Deposited Data		
RNA-seq at d7 of reprogramming of *Adar1*$^{Fl/Fl}$ + Veh (WT) MEFs (biological duplicate)	This study	GEO: GSE130310
RNA-seq at d7 of reprogramming of *Adar1*$^{Fl/Fl}$ + 4OHT (KO) MEFs (biological duplicate)	This study	GEO: GSE130310
RNA-seq at d7 of reprogramming of *Adar1*$^{Fl/E861A}$ + Veh (HET) MEFs	This study	GEO: GSE130310
RNA-seq at d7 of reprogramming of *Adar1*$^{Fl/E861A}$ +4OHT (MUT) MEFs	This study	GEO: GSE130310
Experimental Models: Cell Lines		
Pou5f1-GFP mouse embryonic fibroblasts (MEFs)	This study	N/A
Nanog-GFP MEFs	This study	N/A

(*Continued on next page*)

Please cite this article in press as: Guallar et al., ADAR1-Dependent RNA Editing Promotes MET and iPSC Reprogramming by Alleviating ER Stress, Cell Stem Cell (2020), https://doi.org/10.1016/j.stem.2020.04.016

Continued

REAGENT or RESOURCE	SOURCE	IDENTIFIER
Normal human fetal lung fibroblasts (MRC-5)	ATCC	CCL-171
Peripheral Blood Mononuclear cells (PBMCs)	This study	N/A
Adar1$^{Fl/Fl}$ MEFs	This study	N/A
Adar1$^{Fl/E861A}$ MEFs	This study	N/A
Adar1$^{Fl/Fl;Ifih1-/-}$ MEFs	This study	N/A
Adar1$^{Fl/E861A;Ifih1-/-}$ MEFs	This study	N/A
HEK293T	This study	N/A
Plat-E	This study	N/A
NMuMG	ATCC	CRL-1636
Experimental Models: Organisms/Strains		
C57BL/6 Mouse *Adar1*$^{E861A/+}$: *Adar*$^{tm1.1Xen}$	St. Vincent's Hospital, Melborune	N/A
C57BL/6 Mouse *Ifih1*$^{-/-}$: *Ifih1*$^{tm1.1Cln}$	St. Vincent's Hospital, Melborune	N/A
C57BL/6 Mouse *Adar1*$^{Fl/Fl}$: *Adar1*$^{tm1.1Phs}$	St. Vincent's Hospital, Melborune	N/A
C57BL/6 Mouse Rosa26-CreER^{T2}: (*Gt(ROSA)26*$^{Sortm1(cre/ERT2)Tyj}$)	St. Vincent's Hospital, Melborune	N/A
Oligonucleotides		
For Mouse qPCR primers see Table S4	This study	N/A
For A-to-I RT-qPCR primers see Table S4	This study	N/A
For Dnajc1 PCR for Sanger sequencing see Table S4	This study	N/A
For short hairpin RNAs see Table S4	This study	N/A
For cloning primers see Table S4	This study	N/A
Recombinant DNA		
A-to-I reporter plasmid	Laboratory of Michael Jantsch	N/A
pLKO-shRNA *Luciferase*	This study	N/A
pLKO-shRNA Adar1#1 (mouse)	This study	N/A
pLKO-shRNA Adar1#2 (mouse)	This study	N/A
pLKO-shRNA Adar1#3 (human)	This study	N/A
pLKO-shRNA Adar1#4 (human)	This study	N/A
pLKO-shRNA Adar2#1	This study	N/A
pLKO-shRNA Adar2#2	This study	N/A
pLKO-shRNA Ddx58	This study	N/A
pLKO-shRNA Ifih1	This study	N/A
pLKO-shRNA Mavs	This study	N/A
pLKO-shRNA Atf6	This study	N/A
pLKO-shRNA Ire1	This study	N/A
pLKO-shRNA Atf3	This study	N/A
pLKO-shRNA Herpud1	This study	N/A
pLKO-shRNA Dr5	This study	N/A
pLKO-shRNA Trb3	This study	N/A
pMX-Atf4	This study	N/A
pMX-Jdp2	Laboratory of Dr. Pei (Liu et al.,2015)	N/A
pMX-Jhdm1b	Laboratory of Dr. Pei (Liu et al.,2015)	N/A
pMX-Mkk6	Laboratory of Dr. Pei (Wang et al.,2019)	N/A
pMX-Glis1	Laboratory of Dr. Pei (Wang et al.,2019)	RRID:Addgene_30166
pMX-Nanog	Laboratory of Dr. Pei (Wang et al.,2019)	N/A
pMX-Esrrb	Laboratory of Dr. Pei (Wang et al.,2019)	N/A
pMX-Sall4	Laboratory of Dr. Pei (Liu et al.,2015)	N/A
pMX-EV	This study	N/A

(*Continued on next page*)

Please cite this article in press as: Guallar et al., ADAR1-Dependent RNA Editing Promotes MET and iPSC Reprogramming by Alleviating ER Stress, Cell Stem Cell (2020), https://doi.org/10.1016/j.stem.2020.04.016

Continued

REAGENT or RESOURCE	SOURCE	IDENTIFIER
pMX-Dnajc1	This study	N/A
pMX-Sppl2a	This study	N/A
pMX-Gla	This study	N/A
pMX-Cds2	This study	N/A
pMX-Nol10	This study	N/A
LeGO-iG2#Adar1	Laboratory of Dr. Carl Walkley	N/A
LeGO-iG2#Adar1 E861A	Laboratory of Dr. Carl Walkley	N/A
FUW-TetO-Ascl1	Laboratory of Dr. Wernig (Vierbuchen et al., 2010)	RRID:Addgene_27150
FUW-M2rtTA	This study	N/A
Software and Algorithms		
Bowtie2 v2.3.0	Johns Hopkins University	http://bowtie-bio.sourceforge.net/bowtie2/index.shtml
Bwa v0.5.9	(Li and Durbin, 2009)	https://sourceforge.net/projects/bio-bwa/files/
Cluster v3.0	Stanford University	http://bonsai.hgc.jp/~mdehoon/software/cluster/software.htm#ctv
Cufflinks v2.2.1	Laboratory of Cole Trapnell University of Washington	http://cole-trapnell-lab.github.io/cufflinks/
DAVID functional annotation tool	Laboratory of Human Retrovirology and Immunoinformatics (LHRI)	https://david.ncifcrf.gov/tools.jsp
FlowJo v7.6.1	FlowJo, LLC	https://www.flowjo.com/
GENE-E v3.0.215	Broad Institute	https://software.broadinstitute.org/GENE-E/
GSEA v3.0	Broad Institute	https://www.gsea-msigdb.org/gsea/index.jsp
ImageJ v1.33	NIH	https://imagej.nih.gov/ij/
Leica Application Suite v3.4.2.18368	Leyca Microsystems	https://www.leica-microsystems.com/
mfold v3.6	The RNA Institute	http://unafold.rna.albany.edu/?q=mfold/download-mfold
OriginPro 2017 v9.4.0.220	OriginLab	https://www.originlab.com/Origin
OriginPro 2019b v9.6.5.169	OriginLab	https://www.originlab.com/Origin
Prism v8.0.2	GraphPad	https://www.graphpad.com/
Samtools v0.1.18	(Li et al., 2009)	https://github.com/samtools/samtools
Sequencher v5.4	Gene Codes Corporation	http://www.genecodes.com/
SOAPnuke v1.5.6	BGI	https://github.com/BGI-flexlab/SOAPnuke
TopHat v2.1.1	Johns Hopkins University	https://ccb.jhu.edu/software/tophat/index.shtml
Other		
PRIMER1: primer design for tetra-primer ARMS-PCR	(Ye et al., 2001)	http://primer1.soton.ac.uk/primer1.html
TMHMM Server v. 2.0	DTU Bioinformatics	http://www.cbs.dtu.dk/services/TMHMM/

RESOURCE AVAILABILITY

Lead Contact

Further information and requests for resources and reagents should be directed to and will be fulfilled by the Lead Contact, Jianlong Wang (jw3925@cumc.columbia.edu).

Please cite this article in press as: Guallar et al., ADAR1-Dependent RNA Editing Promotes MET and iPSC Reprogramming by Alleviating ER Stress, Cell Stem Cell (2020), https://doi.org/10.1016/j.stem.2020.04.016

Materials Availability

All unique/stable reagents generated in this study are available from the Lead Contact with a completed Materials Transfer Agreement.

Data and Code Availability

The RNA-seq datasets generated during this study are available at NCBI Gene Expression Omnibus GEO: GSE130310.

EXPERIMENTAL MODEL AND SUBJECT DETAILS

Mice

All animal experiments were approved by the St. Vincent's Institute, Melbourne Animal Ethics Committee (AEC#031/15). *Adar1*$^{E861A/+}$ (*Adar1*$^{E861A/+}$; MGI allele: *Adar*$^{tm1.1Xen}$; MGI:5805648), *Ifih1*$^{-/-}$ (*Ifih1*$^{tm1.1Cln}$), *Adar1*$^{Fl/Fl}$ (*Adar1*$^{Fl/Fl}$; MGI allele: *Adar1*$^{tm1.1Phs}$; MGI:3828307), and Rosa26-CreER^{T2} (*Gt(ROSA)26*$^{Sortm1(cre/ERT2)Tyj}$) mice were on a backcrossed C57BL/6 background as previously described (Heraud-Farlow et al., 2017).

Cells

E13.5 embryos were used to isolate fibroblasts (MEFs). Fibroblasts were maintained in high-glucose DMEM (Dulbecco's modified Eaglés medium, Corning, 10-013-CVR), containing 10% fetal bovine serum (FBS, GIBCO 10270-106), 2 mM L-Glutamine (GE Healthcare, SH30034.01) and 1% penicillin and streptomycin (GIBCO,15140). Cell identity was authenticated by PCR of genomic DNA.

Mouse iPSC lines were maintained on gelatin-coated plates with medium containing high-glucose DMEM, 15% fetal bovine serum, 0.1 mM 2-mercaptoethanol (Sigma Aldrich, M6250), 2 mM L-glutamine, 0.1 mM non-essential amino acids (GIBCO, 11140), 1% of nucleoside mix (Adenosine: Sigma-Aldrich, A4036; Cytidine: Sigma-Aldrich, C4654; Thymidine: Sigma-Aldrich, T1895; Guanosine: Sigma-Aldrich, G6264), 1% penicillin and streptomycin and 1000 U/ml of recombinant leukemia inhibitory factor (LIF). For serial passage, iPSCs were grown in the presence of LIF, and split every other day to maintain 50% confluence.

All cells were cultured at 37°C with 5% CO_2.

METHOD DETAILS

shRNA Design and pMX-Based Retroviral Constructs

The specific shRNAs for knockdown of the genes indicated in the Key Resources Table were designed, synthesized, and subcloned into pLKO.1 vectors (Addgene) expressing puromycin or hygromycin resistance genes as previously described (Lee et al., 2012a). All shRNA constructs were confirmed by sequencing and knockdown efficiency was validated by RT-qPCR. The cDNAs of *Atf4, Dnajc1, Cds2, Sppl2a, Gla* and *Nol10* were PCR amplified from total RNA, cloned into pMX-based retroviral vectors and validated by Sanger sequencing. The target sequences of the shRNAs and the primers for CDS amplification used in this study are provided in Table S4.

Viral Production

Lentiviral pLKO shRNA-expressing vectors and LeGO and FUW transgene-overexpressing vectors were co-transfected with psPAX2 and pMD2.G packaging vectors into HEK293T cells. Retroviral pMX transgene-overexpressing constructs were transfected into Plat-E cells. Briefly, HEK293T and Plat-E cells were maintained in high-glucose DMEM supplemented with 10% FBS, 2 mM L-glutamine, and 1% penicillin and streptomycin. Cells were plated at a density of 8 × 10^6 cells per 150 mm dish to be transfected 24 hours later with PEI (Polyethylenimine; Sigma-Aldrich, 408727) and either 20 μg of pLKO.shRNA, LeGO or FUW plasmids along with 10 μg of psPAX2 and pMD2.G packaging mix or 20 μg of pMX vectors alone. Twenty-four hours later medium was changed, and virus-containing supernatants were collected 48h and 72h post transfection and concentrated using centrifugal filter units with 0.22 μm pore size (Amicon, UFC903024).

OSKM Reprogramming Assays in Somatic Cells to Form iPSCs

Mouse embryonic fibroblasts (MEFs) containing a *Pou5f1*-GFP reporter were infected with lentivirus containing the indicated shRNA and selected with 2 μg/ml puromycin (Fisher Bioreagents, BP2956-100) or 250 μg/ml hygromycin (Corning, 30-240-R). Once selection was completed, transduced MEFs were seeded at a density of 20,000 cells per well of a 12-well plate except for the low-density experiments (i.e., 5.000, 2.500, 1.250 and 625 MEFs were seeded instead). On the next day, cells were infected with lentiviral particles containing a *Pou5f1*, *Sox2*, *Klf4* and *Myc* (OSKM) expression cassette. Twenty-four hours after infection, medium was switched to iPSC medium and RNA or protein samples were collected at the indicated time points. *Pou5f1*-GFP$^+$ colonies were scored at the indicated time points during reprogramming.

R26-CreER^{T2} *Adar1*$^{Fl/Fl}$, *Adar1*$^{Fl/E861A}$, *Adar1*$^{Fl/Fl}$ *Ifih*$^{-/-}$ and *Adar1*$^{Fl/E861A}$ *Ifih*$^{-/-}$ MEFs were treated with 100 ng/ml of 4-hydroxy-tamoxifen (Sigma-Aldrich, H7904) during the whole reprogramming or at the indicated time windows and OSKM reprogramming was carried out and analyzed as described above. To investigate the consequences of ADAR1 WT/E861A rescue or DNAJC1, CDS2, SPPL2A, GLA or NOL10 overexpression during OSKM reprogramming, *Adar1*$^{Fl/Fl}$ MEFs were infected with LeGO lentiviral

Please cite this article in press as: Guallar et al., ADAR1-Dependent RNA Editing Promotes MET and iPSC Reprogramming by Alleviating ER Stress, Cell Stem Cell (2020), https://doi.org/10.1016/j.stem.2020.04.016

or pMX-based retroviral factors, respectively. Alkaline-phosphatase (AP) stained colonies were scored at the indicated time points.

Normal human fetal lung fibroblasts (MRC-5) were transduced with shRNAs against human *ADAR1* (sh*ADAR1*#3 or sh*ADAR1*#4) or an shRNA against *Luciferase* as a control and selected with puromycin. Once selection was completed, cells were seeded on feeders (i.e., mitomycin C-treated MEFs) and infected with OSKM expressing vectors. Next day, cells were switched to human mTeSR iPSC medium (StemCell Technologies, 05826 supplemented with 05827) to initiate reprogramming. Medium was changed every other day. At the end of reprogramming, iPSC colonies were determined by staining against human NANOG (Santa Cruz, sc-374103).

To address ADAR1 requirement for reprograming of somatic cells other than fibroblasts, peripheral blood mononuclear cells (PBMCs) were isolated from mouse whole blood using RBC Lysis Buffer (Alfa Aesar, J62150.AK) and Ficoll-Paque Premium 1.084 (Sigma-Aldrich, GE17-5446-02) following manufacturer's instructions. Reprogramming of PBMCs was performed as previously described (Eminli et al., 2009; Staerk et al., 2010) with some modifications. Briefly, PBMCs were infected with lentiviruses containing Luciferase control or shRNAs directed against *Adar1* and selected with 3 μg/ml puromycin. Once selection was completed, 50,000 transduced PBMCs were transferred onto 12 well plate with feeders (i.e., mitomycin C-treated MEFs) and infected with OSKM expressing vectors. Cytokine supplemented iPSC medium was switched every other day and AP+ colonies were scored at day 19 of reprogramming.

To investigate the effect of *Adar1* depletion on epithelial somatic cell reprogramming, normal murine mammary gland (NMuMG) cells were transduced with shRNAs against *Adar1* or *Luciferase* and OSKM reprogramming was performed as indicated for MEFs above. Quantification of NANOG+ cells at day 14 of reprogramming was performed by flow cytometry analysis.

7 Factor Reprogramming Assays in Fibroblasts to Form iPSCs

Reprogramming in presence of 7 Factor (7F) cocktail combination (i.e., JDP2, JHDM1B, MKK6, GLIS1, NANOG, ESSRB and SALL4) was performed as previously described (Wang et al., 2019). Briefly, MEFs were seeded at a density of 20,000 cells per 12-well plates. Twenty-four hours after seeding, cells were infected with both shRNAs constructs against *Luciferase* and *Adar1*, and the viral supernatants of the 7F overexpressing vectors. The following day, medium was switched to pluripotent stem cell medium (iSF1). Medium was changed every other day and iPSC colonies were stained with alkaline phosphatase and scored at day 18 of reprogramming.

Reprogramming Assays Using Reprogramming Intermediates

MEF reprogramming intermediates were isolated as previously described (Costa et al., 2013). Briefly, MEFs carrying a GFP reporter under the control of the pluripotency marker *Nanog* (*Nanog*-GFP) were infected with pMX-based retroviral reprogramming factors (OSKM), and cultures were switched to iPSC medium at day 3 post transduction. A clonal line of proliferative, GFP-negative cells (pre-iPSCs, which represent reprogramming intermediates), was transfected using Lipofectamine 3000 Reagent (Invitrogen, L3000-015) with a PiggyBac empty vector or a PiggyBac coding for NANOG. Stable transgene expression was selected with hygromycin for a minimum of 12 days. After selection, cells were infected with lentiviruses containing *Luciferase* control or shRNAs directed against *Adar1* and selected with 1 μg/ml puromycin. Fifty-thousand pre-iPS cells expressing shRNAs were seeded onto 12-well plates and 24h later medium was switched to 2i+LIF medium, which consisted of dual inhibition of mitogen-activated protein kinase signaling (PD0325901, 1 μM) and glycogen synthase kinase-3 (GSK3) (CHIR99021, 3 μM) and LIF. *Nanog*-GFP^{+} colonies from MEF reprogramming intermediates were scored at day 10 of reprogramming.

Direct Reprogramming to Neurons

Direct reprogramming (also known as transdifferentiation) of MEFs to induced neurons (iN) was performed following a previously published protocol (Chanda et al., 2014; Vierbuchen et al., 2010). Briefly, MEFs transduced with shRNAs against *Luci* or *Adar1* and selected with puromycin were seeded at a density of 5,000 cells per 48-well plates. Next day, cells were transfected with a doxycycline inducible FUW-TetO plasmid expressing *Ascl1* factor together with the FUW-M2rtTA vector. Twenty-four hours later, medium was changed to N3B27, which consists in N2B27 supplemented with insulin (5 μg/ml) (Sigma-Aldrich, I2643), and in presence of 2 μg/ml doxycycline. Medium was changed every other day. At day 12 of transdifferentiation, cells were stained with anti-TUJ1 antibody (GeneTex, GTX631836). Pictures were taken at 4X magnification and the number of TUJ1+ cells per field was quantified in 15 random fields per condition.

iPSC Differentiation Assays

Adar$^{Fl/Fl}$ MEFs were reprogrammed with OSKM and iPSC clones were picked. After treatment with vehicle or 4-hydroxytamoxifen (4OHT) for several passages, recombination of the floxed alleles was confirmed by PCR of genomic DNA. Mesendoderm differentiation of iPSCs was performed following a previous published protocol with minor modifications (Thomson et al., 2011). Briefly, iPSCs were maintained and passaged on gelatin-coated plates in N2B27 media supplemented with LIF, BMP4 (10ng/μl) and PD0325901 (1 μM) for a minimum of 4 days. Cells were then seeded at a density of 15,000 cells/cm^2 in N2B27. After 48 hours, medium was replaced with N2B27 supplemented with CHIR99021 (3 μM) to drive lineage specific differentiation. Thirty-six hours later, RNA was collected and RT-qPCR was performed as described below.

Embryoid body differentiation of iPSCs was performed as previously described (Doetschman et al., 1985). In brief, 155,000 cells per mL were seeded in low attachment plates and cultured at 37°C with 5% CO_2 in iPSC standard medium without LIF. Medium was changed every other day. RNA was collected at the indicated time points and RT-qPCR was performed as described below.

Please cite this article in press as: Guallar et al., ADAR1-Dependent RNA Editing Promotes MET and iPSC Reprogramming by Alleviating ER Stress, Cell Stem Cell (2020), https://doi.org/10.1016/j.stem.2020.04.016

Determination of Cell Death

Cells transduced with shRNAs against *Adar1* or *Luciferase* control were collected at the indicated time points during OSKM reprogramming to analyze cell viability. On the one hand, cellular death was determined by trypan blue exclusion assay. Briefly, cells were stained with trypan blue solution (0.08%) (Amresco, K940) at specific times of reprogramming. Live cells versus dead cells (blue) were counted under the microscope and the percentage of each population was represented. On the other hand, cellular apoptosis was determined by flow cytometry using the Dead Cell Apoptosis kit with Annexin V Alexa Fluor 488 (Life Technologies, 10652071) following manufacturer's instructions. As a positive control, some wells of each shRNA treatment were treated with 1 μM staurosporine (Sigma-Aldrich, S5921) to induce apoptosis, or DMSO as control. Flow cytometry was performed using an Accuri C6 instrument (BD Biosciences), and data were analyzed with FlowJo software.

Treatment with Endoplasmic Reticulum Stress Inducers and Inhibitors

MEFs were subjected to reprogramming through lentiviral OSKM expression and 24 hours later were treated with ER stress inducers [i.e., 0.1μg/ml Tunicamycin (Sigma-Aldrich, T7765) or 0.1 μM Thapsigargin (Tocris, 1138)] or ER stress alleviators [i.e., 1 μM of Salubrinal (Cayman, 14735), 1 μM Azoramide (Cayman, 18045)] at the indicated times during reprogramming. ER stress was also genetically reduced by overexpression of ATF4 or wild-type GRP78 or induced by overexpression of a GRP78-dominant negative (GRP78/BiP-DN) (Contreras et al., 2014; Martinez-Sanchez et al., 2017).

Western Blot Analysis and Quantification

Whole cell extracts were obtained by homogenization of cellular pellets in lysis buffer containing 0.05 M Tris-HCl, 0.01 M EGTA, 0.001 M EDTA, 0.016 M Triton X-100, 0.001 M sodium orthovanadate, 0.05 M sodium fluoride, 0.01 M sodium pyrophosphate and 0.25 M sucrose (pH adjusted to 7.5) with freshly added protease inhibitors (Sigma-Aldrich, P8340). After homogenization, samples were centrifuged 10 min at 10,000 g at 4°C to remove cellular debris. Protein samples were prepared by adding Laemmli buffer and denatured by boiling at 95°C for 5 min. Protein extracts were resolved in NovexWedgeWell 4%–20% Tris-Glycine Gels (Invitrogen, XP04205BOX). The following antibodies were used for blotting: ACTB (Santa Cruz, sc-47778), ATF6α (Santa Cruz, sc-22799), β-TUBULIN (Santa Cruz, sc-55529), CDH1 (BD Biosciences, 610182), CDH2 (Santa Cruz, sc-393933), CHOP (Santa Cruz, sc-793), c-FOS (Santa Cruz, sc-52), c-JUN (Santa Cruz, sc-74543), MDA5 (ProteinTech, 21775-1-AP), NANOG (Bethyl Laboratories, A300-397A), pEIF2α (Santa Cruz, sc-101670), pIRE (Abcam, ab48187), PERK (Cell Signaling, #31925) and pPERK (Cell Signaling, #3179),

For western blotting quantification, autoradiographic films were scanned and the band signal was quantified by densitometry using the Image-J-1.33 software (NIH; Bethesda, MD, USA). Values obtained were expressed compared to ACTB or β-TUBULIN as indicated.

Immunofluorescence

Cells were seeded in 48-well plate coated with gelatin 0.1% (w/v). Immunofluorescence was performed at day 7 of the OSKM reprogramming process or at day 12 of transdifferentiation assay. Briefly, cells were fixed with 4% paraformaldehyde (w/v) for 15 min at room temperature for all antibodies except anti-β TUBULIN, where 100% methanol was used for 10 min at −20°C. After fixation, cells were blocked and permeabilized with 2% (w/v) BSA and 0.1% (v/v) Triton X-100 diluted in Dulbecco's phosphate buffered saline (PBS) for 1 hour at RT. For immunostaining, cells were incubated overnight with primary antibodies against CDH1 (BD, 610182), SSEA1 (Thermo Fisher, MA1-022-D488), TUJ1 (GeneTex, GTX631836) and β-TUBULIN (Santa Cruz, sc-55529) in PBS with 2% BSA (w/v) and 0.1% Triton X-100 (v/v). The next day, cells were incubated with fluorophore-labeled secondary antibodies, together with 4'-6-diamidino-phenylindole (DAPI) diluted in PBS with 2% BSA (w/v) and 0.1% Triton X-100 (v/v) for 1 h at room temperature. Immunofluorescence images were taken with a Leica DMI 6000 inverted microscope at 4x or 40x magnification, and image settings were maintained at constant levels for each set of images acquired per factor stained.

Alkaline Phosphatase (AP) Staining

AP staining was measured using an alkaline phosphatase kit (Sigma-Aldrich, 86R-1KT) following the manufacturer's recommendations.

Colony Formation Assay

Adar1$^{Fl/Fl}$ iPSCs were obtained through reprogramming of *Adar1*$^{Fl/Fl}$ MEFs by lentiviral OSKM expression, and then treated with 4OHT or control (Veh) for several passages. iPSCs were seeded at low density (500 cells per well of a 6-well plate) in triplicates on gelatin-coated wells. iPSCs were maintained in culture in presence of regular iPSC medium. Cells were stained for alkaline phosphatase (AP) activity, as a pluripotency indicator. Undifferentiated (alkaline positive), partially differentiated (low AP signal) and differentiated (negative staining) colonies were scored after 6 days of culture.

RNA Extraction and Analysis by Quantitative PCR (RT-qPCR)

RNA was extracted using the E.Z.N.A Total RNA Kit I (Omega, R6834-02) and total RNA was converted into cDNA using qSCRIPT (Quanta, 84034) following manufacturer's instructions. Quantitative PCR was performed using the Fast SYBR® Green Master Mix (Applied Biosystems, A25742) on the StepOnePlus Real-Time PCR System (Applied Biosystem). Data was analyzed using the

delta-delta CT method, which was normalized to the values of a housekeeping gene. Then, the relative expression values were further normalized to the values generated from indicated control samples. Gene-specific primers used for this study are provided in Table S4.

Analysis of Membrane and Cytoplasmic Fractions

MEFs were subjected to reprogramming with OSKM lentiviral system and membrane and cytosol RNA fractions were prepared using a previously published protocol (Jagannathan et al., 2011). Briefly, at day 7 of reprogramming, cells were washed with PBS and treated with 50 μg/ml Cycloheximide (CHX, VWR, 94271) in ice-cold PBS for 10 min on ice. Cells were then permeabilized with permeabilization buffer (110 mM KOAc, 25 mM K-HEPES pH 7.2, 2.5 mM $Mg(OAc)_2$, 1mM EGTA, 0.015% digitonin (w/v), 1 mM DTT, 50 μg/ml CHX, 1x Protease Inhibitor Cocktail (Sigma-Aldrich, P8340), 40 U/ml RNase OUT (Invitrogen, 10777019) for 5 min at 4°C, and cytosolic RNA fraction was collected. Plates were then washed with wash buffer (110 mM KOAc, 25 mM K-HEPES pH 7.2, 2.5 mM $Mg(OAc)_2$, 1 mM EGTA, 0.004% digitonin (w/v), 1 mM DTT, 50 μg/ml CHX) and treated with lysis buffer (400 mM KOAc, 25 mM K-HEPES pH 7.2, 15 mM $Mg(OAc)_2$, 1% (v/v) NP-40, 0.5% (w/v) Sodium Deoxycholate,1 mM DTT, 50 μg/ml CHX, 1x Protease Inhibitor Cocktail, 40 U/ml RNase OUT) for 5 min at 4°C. Membrane RNA fraction was then collected, and both fractions were clarified by centrifugation at 7,500 g for 10 min at 4°C, to remove cell debris. RNA was then extracted with Direct-zol RNA Miniprep Plus kit (Zymo Research, R2070) following manufacturer's protocol and RT-qPCR was performed as described above.

For extracting membrane and cytosolic protein fractions a similar protocol was followed, including the addition to the permeabilization and lysis buffers of benzonase nuclease (Sigma, E1014-5KU) to remove DNA and RNA. Both fractions were used in Western Blot, which was performed following the protocol described above.

In Vitro RNA Immunoprecipitation (iv-RIP)

IV-RIP was performed as we previously described (Guallar et al., 2018) with some modifications. Total protein extracts were obtained by incubation of MEF cell pellets with lysis buffer (150 mM NaCl, 10 mM Tris-HCl pH7.4, 1 mM EDTA, 1 mM EGTA, 0.2 mM Sodium Orthovanadate, 0.2 mM PMSF, 1% Triton X-100 (v/v), 0,5% NP-40 (v/v), 1X protease inhibitor cocktail, RNase OUT, RNase IN) for 30 min at 4°C in constant rotation. For whole cell extract preparation, samples were sonicated with a Branson sonicator (4 cycles [5 s ON, 30 s OFF] at 50% amplitude), and insoluble elements were cleared by centrifugation at 4,000 g for 30 min at 4°C. Protein concentration was measured with Bradford reagent (Sigma-Aldrich, B9616), and 1 mg of total protein was used for immunoprecipitation in LoBind protein tubes (Eppendorf, 0030108132). One percent of protein was kept as input sample. For the immunoprecipitation, the reaction volume was brought to 1.5 mL and NaCl was adjusted to 100 mM by adding lysis buffer without NaCl. Then, 2 μg of antibody [IgG (Millipore, 12-371) or anti-MDA5 (ProteinTech, 21775-1-AP)], 2 μl of Benzonase (Sigma-Aldrich, E1014-5KU) and $MgCl_2$ to a final concentration of 1.5mM were added to the reaction. Immune complexes were allowed to form overnight at 4°C in constant rotation.

Total RNAs (from *Adar1*$^{Fl/Fl}$ treated with vehicle or 4OHT) were subjected to Proteinase K (Thermo Scientific, EO0491) and DNase I (Thermo Fisher, EN0521) treatment, and then fragmented for 1 min at 95°C using NEBNext Magnesium RNA Fragmentation Module (NEB, 6186A), to obtain fragments of around 1000 bp. RNA was precipitated with NaAc (pH5.2) and ethanol. RNA pellets were resuspended in nuclease-free water.

To collect immunocomplexes, Dynabeads Protein G (Invitrogen, 10004D) were added and incubated 2 h in constant rotation at 4°C. Beads were then washed five times with lysis buffer with 100 mM NaCl and resuspended in RNA immunoprecipitation (RIP) buffer [150 mM KCl, 25 mM Tris-HCl pH7.5, 5 mM EDTA, 0.5% NP-40 (v/v)] with protease and RNase inhibitors. 600 ng of total fragmented RNA was added to beads-protein complexes and incubated by gentle rotation for 45 min at room temperature. Beads containing the RNA-protein complexes were washed five times with RIP buffer and RNA was eluted with TRIzol, following manufacturer's instructions. Immunopurified RNAs were analyzed by RT-qPCR as described above.

RNA Sequencing (RNA-seq) and Analysis

Total RNA was extracted using Phasemaker tubes (Invitrogen, 15642268) and TRIzol reagent (Invitrogen, 15596026), subjected to a RiboZero selection protocol following the manufacturer's instructions and paired-end sequencing was carried out with the Illumina HiSeq4000 with read length of 150 bp. Biological replicates of *Adar1*$^{Fl/Fl}$ + Veh and *Adar1*$^{Fl/Fl}$ + 4OHT, *Adar1*$^{Fl/E861A}$ + Veh and *Adar1*$^{Fl/E861A}$ + 4OHT samples at day 7 of OSKM reprogramming were subjected to sequencing. Reads were aligned to the mouse genome (GRCm38, mm10) using TopHat (v2.1.1) and Bowtie2 (v2.3.0) with the default parameter settings. Assembly of novel transcripts was not allowed (-G) and other parameters were used following default settings. Transcript assembly and differential expression analysis were performed by Cufflinks (v2.2.1), and expression of transcripts sharing each gene_id was quantified as Fragments Per Kilobase Million (FPKM). Significance of differential expression was determined with the Benjamini-Hochberg correction for multiple testing.

Hierarchical clustering of RNA-seq samples used in this study was performed using GENE-E 3.0.215. The datasets were grouped using the Pearson correlation coefficient (R), clustering the distance with average linkage. Genes not expressed were filtered out.

Gene Set Enrichment Analysis (GSEA)

GSEA (v3.0, available at https://www.gsea-msigdb.org/gsea/index.jsp) was used to assess the statistically enriched differences between the indicated samples. Briefly, the software was run with 1000 as permutation number and a gene_set permutation

Please cite this article in press as: Guallar et al., ADAR1-Dependent RNA Editing Promotes MET and iPSC Reprogramming by Alleviating ER Stress, Cell Stem Cell (2020), https://doi.org/10.1016/j.stem.2020.04.016

type was used. Enrichment analysis was weighted _p2 for the enrichment score calculation, and t test was used to rank genes. Enrichment plot, normalized enrichment score (NES), statistical significance (*P*-value) and False Discovery Rate (FDR) were calculated using the software.

RNA Editing Detection from Mouse RNA-seq Data

To detect RNA editing sites from mouse RNA-seq data, we developed a custom pipeline based on our previously reported pipeline for analyzing A-to-I editing in human samples (Xiong et al., 2017). First, RNA read cleaning was performed with SOAPnuke (v1.5.6) to filter low-quality reads (more than 50% sequencing bases with quality < 5 in a read), reads containing adaptor sequences and those with more than five unknown (N) bases. If one read of a read pair was filtered out, the other one would be discarded as well. In order to use BWA to map RNA-seq data, we then built a new reference which combines the mouse reference genome (mm10) and transcriptome, created by concatenating exonic sequences surrounding all known splice junctions (downloaded from ftp://ftp.ensembl.org/pub/release-94/gtf/mus_musculus), as previously described (Ramaswami et al., 2012; Wang et al., 2016).

The high-quality pair-end reads were mapped to the combined reference created in the previous step, using BWA (v 0.5.9, http://bio-bwa.sourceforge.net/) with parameters: -l -k 3 -l 32 -n 0.08. After BWA alignment, the locations of reads mapped to junction sequences were converted back to regular genomic coordinates before subsequent analysis. Then, PCR duplicates were removed by samtools (samtools-0.1.18, https://sourceforge.net/projects/samtools/files/samtools/0.1.18/). Variants were detected by an in-house developed tool (MutDet) based on pileup information from RNA read alignment, which extracts various features based on RNA-seq reads to facilitate variant filtering in the next step.

Finally, variant filtering was performed to identify RNA-editing sites based on the variants called in the previous step. We only kept uniquely mapped reads and checked those positions having reads with base-quality $\geq$ 20. We further filtered variants based on the criteria explained below, and those that passed all filters were considered as bona fide RNA editing sites. The first four steps were accomplished by a Perl script "binom.reads.fre.end.strand.mism.poly.rep.filter.pl" and the last step was attained by "snp.filter.pl."

Criteria for Variant Filtering

(1) We performed statistical test based on binomial distribution B (n, p) to distinguish true variants from those due to sequencing errors on every mismatch site, where p denotes the background mismatch rate of each transcriptome, and n denotes sequencing depth on this site. On a specific site with k reads supporting variant in all n mapped reads, we used B (k, n, p) to calculate the probability that the k mismatches are all due to sequencing errors. This probability is adjusted using the Benjamini-Hochberg method. We retained sites with adjusted *P*-value < 0.01, number of mapped reads $\geq$ 4, variant-supporting reads $\geq$ 2, and mismatch frequencies (variant-supporting-reads/mapped-reads) $\geq$ 0.1.

(2) We estimated strand bias and filtered out variants with strong strand bias as follows:

(a) We performed a two-tailed Fisher's exact test using the following two-by-two table:

	Variant supporting reads	Reference supporting reads
Sense strand	Sense strand variant supporting reads	Sense Strand reference supporting reads
Antisense strand	Antisense strand variant supporting reads	Antisense strand reference supporting reads

(b) We estimated variant strand frequency (sense-strand variant-supporting reads divided by total variant-supporting reads), variant strand preference [absolute (variant strand frequency minus 0.5)], reference strand frequency (sense-strand reference minus supporting read number divided by total reference-supporting read number), and reference strand preference [absolute (reference strand frequency minus 0.5)].

(c) We filtered out variant sites displaying significant strand bias, defined as either Fisher's exact test *P*-value < 0.005 plus variant strand preference > reference strand preference, or variant strand frequency > 0.9, or variant strand frequency < 0.1.

(3) We estimated and filtered out variants with position bias, defined as either Fisher's exact test *P*-value < 0.05 plus read end frequency > read middle frequency, or read end frequency > 0.9. We defined a read-end as 10bp at 3′ end or 5bp at 5′ end.

(4) We removed variant sites that are in simple repeat regions (http://hgdownload.cse.ucsc.edu/goldenPath/mm10/database/), or in homopolymer regions (runs of $\geq$ 5 bp).

5) Finally, candidate variants were filtered out if they were found in the combined SNP database (ftp://ftp-mouse.sanger.ac.uk/current_snps/).

Comparison of Editing Levels in MEF and iPSC Samples

To determine the editing levels in MEFs and iPSCs, we selected sites that were covered by at least 3 supporting reads of the edited form and that were edited at least 10% in any sample. We then focused on sites in which editing could be detected in at least 4 samples of the corresponding cell type. The editing of individual sites was calculated as the number of G reads divided by the total number of A and G reads mapped to an editing site. Mean editing frequency was calculated as the average of all editing of individual sites per sample. All published datasets used in this study are compiled in Table S4.

Please cite this article in press as: Guallar et al., ADAR1-Dependent RNA Editing Promotes MET and iPSC Reprogramming by Alleviating ER Stress, Cell Stem Cell (2020), https://doi.org/10.1016/j.stem.2020.04.016

Principal Component Analysis (PCA) and Gene Ontology (GO)

Principal component analysis was performed to compare editing of MEF and iPSC datasets. Briefly, the expression data matrix was imported by Cluster 3.0 software (http://bonsai.hgc.jp/~mdehoon/software/cluster/), a mean center and gene normalization was applied. Then PCA were applied to arrays and results were virtualized using Origin software (Origin Pro 2017 b9.4.0.220).

Gene ontology analyses were performed using DAVID functional annotation tool (https://david.abcc.ncifcrf.gov/tools.jsp) (Huang da et al., 2009) with a reference list including all *Mus musculus* genes from NCBI. Gene ontologies used for comparative transcriptional analysis in this study are listed below:

GO term	GO ID
epithelial cell development	GO:0002064
endoplasmic reticulum unfolded protein response (UPR)	GO:0030968
response to endoplasmic reticulum stress	GO:0034976
cellular response to topologically incorrect protein	GO:0035967
innate immune response (IIR)	GO:0045087
membrane	GO:0016020
endoplasmic reticulum	GO:0005783
membrane-enclosed lumen	GO:0031974
intracellular membrane-bounded organelle	GO:0043231
membrane-bounded organelle	GO:0043227
response to stress	GO:0006950

Validation of A-to-I Editing by RT-qPCR

We validated editing sites detected *in silico* by performing a RT-qPCR as previously described with some modifications (Ye et al., 2001). Briefly, we designed primers to specifically detect the transcript with the edited variant (G or C). For primer design, we used the online tool http://primer1.soton.ac.uk/primer1.html. Genomic sequences required for the program were downloaded from UCSC Genome Browser (GRCm38/mm10 mouse genome). The following qPCR program was used: 98°C for 10 min, followed by 40 cycles of 95°C for 15 s, 55°C 15 s, 72°C for 40 s, then followed by 95°C, 65°C for 1 min and lastly 97°C for 15 s. Primers used can be found in Table S4.

Validation of Editing by Sanger Sequencing

We used qSCRIPT to obtain cDNA from total RNA from the samples of interest and subjected them to PCR with specific primers to amplify regions containing several editing sites of interest. PCR amplicons were run in a gel and the band of the appropriate size was excised and extracted with GenElute Gel Extraction Kit (Sigma-Aldrich, NA1111). Then, the PCR fragment was either sent for Sanger sequencing or cloned into a pJET1.2 blunt vector with the CloneJet PCR Cloning kit (Thermo Fisher, K1231). Eight clones of each indicated genotype were then sent for Sanger sequencing. All primer sequences can be found in Table S4.

Editing Analysis Using a Reporter System

For detection of RNA editing a previously reported fluorescent reporter system was used (Tariq et al., 2013). Briefly, the reporter plasmid confers resistance to neomycin, and encodes for two fluorescent proteins, GFP and RFP, coupled by a double stranded RNA linker harboring an amber stop codon (UAG) in which the adenosine is susceptible of being A-to-I edited. When this adenosine is deaminated, the codon change to a tryptophan (UGG) allows the expression of GFP, while the RFP fluorescence remains constant.

Fifty thousand MEFs or eighty thousand iPSCs were seeded in a 6-well or 12-well plate, respectively. Next day, MEFs and iPSCs were transfected with 1 or 0.8 μg of the reporter construct (respectively) with transfection reagent following manufacturer's protocol (Polyplus, 114-01). The following day, transfected MEFs or iPSCs were selected using 600 μg/ml and 400 μg/ml of G418 (Corning, 15303681), respectively. Cells were analyzed by flow cytometry three days after transfection in a BD FACScalibur and the ratio between GFP and RFP mean fluorescence intensity was determined.

RNA Secondary Structure Prediction

Genomic sequences from *Mus musculus* GRCm38/mm10 mouse genome were used to predict the RNA secondary structure using the mfold Web Server (http://unafold.rna.albany.edu/?q=mfold). Secondary structure prediction was performed accounting with GU basepairs, and with inosine in place of the edited adenosines identified in our study (assuming no base pairing), as previously described (Liddicoat et al., 2015). Briefly, prediction was performed using RNAfold 3.6 with default settings. For the unedited transcript we supply the non-modified structure of the 3′UTR of *Dnajc1*. For the edited transcripts we replace with "I"s all the "A"s nucleotides in all A-to-I sites detected and validated with our editing analysis.

Transmembrane Domains and ER Signal Peptides Prediction

Uniprot database (https://www.uniprot.org/) was used to predict the transmembrane domains and endoplasmic reticulum (ER) signal peptides. TMHMM prediction software (TMHMM Server v. 2.0) was used to manually curate the proteins that are also predicted to possess transmembrane domains but are not included in Uniprot.

QUANTIFICATION AND STATISTICAL ANALYSIS

All statistical analysis was performed with GraphPad Prism (GraphPad Software, Inc.), Excel or R (http://www.r-project.org/). Statistical significance was identified by Student's t test or one-way ANOVA with Tukey's post-test as indicated in the manuscript or figure legends. *P value*s of less than 0.05 were considered statistically significant. $^{*}p < 0.05$, $^{**}p < 0.01$, $^{***}p < 0.001$, $^{****}p < 0.0001$.